

Unraveling Excitonic Effects for the First Hyperpolarizabilities of Chromophore Aggregates

Aleksey A. Kocherzhenko,^{*,†} Sapana V. Shedje,[‡] Xochitl Sosa Vazquez,[‡] Jessica Maat,[‡] Jacob Wilmer,[‡] Andreas F. Tillack,^{§,⊥} Lewis E. Johnson,^{||} and Christine M. Isborn^{*,‡,||}

[†]Chemistry and Biochemistry, California State University, East Bay, Hayward, California 94542, United States

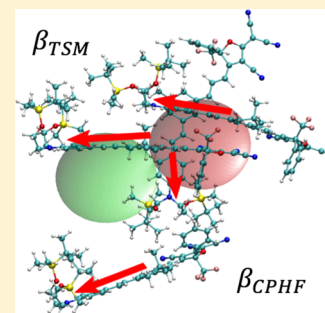
[‡]Chemistry and Chemical Biology, University of California, Merced, Merced, California 95343, United States

[§]Oak Ridge National Laboratory, Oak Ridge, Tennessee 37831, United States

^{||}Department of Chemistry, University of Washington, Seattle, Washington 98195, United States

Supporting Information

ABSTRACT: Excitonic interactions often significantly affect the optoelectronic properties of molecular materials. However, their role in determining the nonlinear optical response of organic electro-optic materials remains poorly understood. In this paper, we explore the effects of excitonic interactions on the first hyperpolarizability for aggregates of donor–acceptor chromophores. We show that calculations of the first hyperpolarizability of chromophore aggregates based on a two-state model agree well with the more rigorous coupled perturbed Hartree–Fock method. We then use both time-dependent density functional theory calculations and the molecular exciton approximation to parametrize the two-state model. Use of the molecular exciton approximation to the two-state model (i) is appropriate for disordered aggregates (unlike band theory), (ii) is computationally efficient enough for calculating the first hyperpolarizability of materials that consist of thousands of interacting chromophores, and (iii) allows the unraveling of the effects of both excitonic interactions and electrostatic polarization of the chromophore electron density by its environment on the first hyperpolarizability of molecular materials. We find that use of the molecular exciton approximation to the two-state model does not introduce significant additional errors compared to those introduced by applying the two-state model alone. We determine that the absolute change to the first hyperpolarizability of chromophore aggregates due to excitonic interactions increases with the size of the aggregate. For all sizes of disordered aggregates of chromophores considered in this paper, the inclusion of excitonic interactions on average decreases the magnitude of the first hyperpolarizability by 12–14% compared to the case of non-interacting chromophores. Finally, we present a method for analytically calculating the first hyperpolarizability of a one-dimensional periodic array of chromophores within the molecular exciton approximation to the two-state model. This technique can be used to include an approximate correction for excitonic effects when simulating the electro-optic response of disordered and ordered organic materials.



1. INTRODUCTION

Organic electro-optic (OEO) materials have the potential for higher operating frequencies and bandwidths, smaller footprints, lower drive voltages, and improved energy efficiency compared with the crystalline inorganic materials currently used for detection and modulation in many optical telecommunications, computing, and sensor technologies.^{1–11} OEO materials typically consist of highly dipolar push–pull (donor–acceptor) chromophores that can easily redistribute electron density upon application of an electric field, leading to large molecular first hyperpolarizabilities. Depending on the material, the chromophores may form amorphous aggregates, whether neat or combined with a polymer, or, less frequently, may form ordered crystals^{12,13} (such as 4-*N,N*-dimethylamino-4'-*N'*-methyl-stilbazolium tosylate^{14,15}). Interchromophore interactions, such as polarization and excitonic effects, could substantially affect the electronic response of the OEO material, as has been shown for organic photovoltaic

materials.^{16–23} A number of studies have demonstrated that the electro-optic response of chromophores is nonadditive.^{24–27} This finding suggests that theoretical models for the hyperpolarizability of chromophore aggregates, films, and solids must account for interchromophore interactions. Computational characterization of the electro-optic response based on such models can provide insights for designing new electro-optic chromophores and optimizing chromophore alignment.^{28,29} Ideally, computational techniques should accurately model the hyperpolarizability of single chromophores, as well as capture interchromophore interactions.

Various electronic structure methods have been used to compute the molecular hyperpolarizability of typical push–pull chromophores.^{30–34} Benchmark studies for hyperpolarizability

Received: December 26, 2018

Revised: February 21, 2019

Published: February 27, 2019



have shown that density functional theory (DFT) methods with large percentages of asymptotic exact exchange provide accurate trends,^{35–37} although the incorrect pole structure in time-dependent DFT (TDDFT) may cause overly resonant hyperpolarizabilities at certain frequencies.³⁸ Good accuracy at a reasonable computational cost makes DFT methods attractive for studying large push–pull chromophores with strong electro-optic response, such as YLD124 (shown in Figure 1), a higher-performance derivative of the prototypical

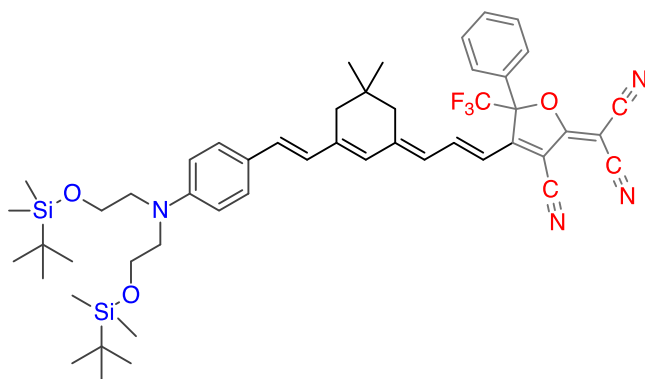


Figure 1. Chemical structure of the YLD124 chromophore. The electron-donating group is diethyl amine with *tert*-butyldimethylsilyl protecting groups (highlighted in blue), and the electron accepting group is 2-(3-cyano-4,5,5-trimethyl-5H-furan-2-ylidene)-malononitrile (highlighted in red).

CLD chromophore³⁹ that forms the basis of most modern OEO chromophores.⁴⁰ However, the cubic scaling of hybrid DFT methods typically restricts their applicability to small chromophore aggregates ($\sim 10^4$ basis functions).

Polarizabilities of periodic systems can be calculated using plane-wave or localized basis codes, such as CRYSTAL.^{41–45} However, periodic DFT codes are generally restricted to the use of nonhybrid (e.g., Perdew–Burke–Ernzerhof)⁴⁶ or screened (e.g., Heyd–Scuseria–Ernzerhof)⁴⁷ density functionals and therefore do not accurately describe charge-transfer excitations or excitonic interactions. Bethe–Salpeter calculations⁴⁸ account for the Coulombic screening of the electron and hole and can improve accuracy, but these calculations are computationally expensive and are generally not feasible for systems where the unit cell contains more than a single chromophore with high hyperpolarizability. The frequency dependence of the nonlinear susceptibility in molecular crystals has been investigated by Munn through the dielectric theory of excitons.⁴⁹ The effects of intermolecular interactions on the electro-optic response of crystalline materials have also been studied using a subsystem approach, where the response is computed for ordered aggregates of increasing size.^{50,51} A charge embedding approach to account for the crystal field effects on the molecular (hyper)polarizabilities has also been developed for periodic systems.^{52–54}

Neither DFT calculations for small chromophore aggregates nor calculations for periodic systems are suitable for analyzing disordered or semioordered chromophore aggregates, as well as significantly disordered molecular films and solids. The electro-optic response of such systems is often represented using a sum of molecular hyperpolarizabilities^{12,55} or a product of the single-molecule hyperpolarizability and an average order parameter.⁵⁶ However, these additive approaches neglect the effects of interchromophore interactions, including exciton

delocalization over multiple chromophores and polarization of the electron density by surrounding chromophores, on the electro-optic response. Developing a method for modeling the hyperpolarizability and electro-optic response of bulk molecular systems is key for theory-assisted rational design of next-generation OEO materials.

The polarizabilities of a single molecule or a very small molecular aggregate can be computed by taking the analytical derivatives of the total molecular energy with respect to the applied electric field within the coupled-perturbed Hartree–Fock (CPHF) formalism.^{57–61} Within DFT, this approach is also referred to as coupled-perturbed Kohn–Sham but we will use the term CPHF throughout this paper. Formally equivalent values of the molecular polarizabilities can be computed using “sum-over-states” expressions that are derived from a perturbation theory treatment of electric fields that interact with the molecule.⁶² In this approach, the polarizabilities are expressed in terms of excitation energies and dipole moment matrix elements for all combinations of excited states. The first molecular hyperpolarizability, usually denoted as β , is unique in that the sum-over-states expression for it can be approximated within a two-state model (TSM) for organic push–pull molecules.^{63,64} The TSM neglects the effects of all excited states beyond the lowest-energy bright state, making the assumption that the first hyperpolarizability, β , is largely determined by the ground- and lowest excited-state properties.

Over the past three decades, the TSM has been used extensively for calculations of the static and dynamic first hyperpolarizabilities of numerous organic molecules.^{65–72} The reliability of the TSM for single molecules has been assessed by comparison to sum-over-states calculations of the first hyperpolarizability, β , using a semiempirical Hamiltonian.^{72–74} It has been found that the TSM reliably reproduces the magnitude of β calculated using sum-over-states expressions with $\approx 80\%$ accuracy. Johnson et al.³⁶ and Muhammad et al.⁷⁵ compared the values of β calculated using various ab initio methods to experimental results extrapolated to the static limit using a TSM. Several studies have also compared the TSM with CPHF.^{67,76,77} Qualitatively, the TSM showed good agreement with CPHF calculations for charge-transfer molecules.^{78,79} Silva et al.⁷⁷ reported that the TSM could reproduce static first hyperpolarizability values calculated using CPHF with variations of only 5% between the two methods. Paschoal et al.⁸⁰ also reported good agreement between static and dynamic β values calculated using CPHF and the TSM for a set of organic push–pull molecules. Moreover, their analysis confirms that charge transfer between the ground and lowest bright excited state could be responsible for more than 99% of the second-order response.

In contrast, other studies have reported failure of the TSM to quantitatively predict the first hyperpolarizability.^{81–83} Vivas et al.⁸⁴ observed poor agreement between the β values calculated using CPHF and the TSM for molecules with octupolar character. The TSM does not adequately capture the nonlinear response of such molecules, so the use of a three-level model is essential. Benassi et al.⁶⁷ found large discrepancies between CPHF and the TSM for cationic molecules, possibly due to solvent effects. Silva et al.⁷⁷ observed variations of 20–27% between the dynamic first hyperpolarizability values calculated using CPHF and the TSM that are a consequence of CPHF poorly describing β enhancement near the electronic resonances. Using damped

dispersion within the TSM led to significant improvement in the calculated dynamic first hyperpolarizability.

Despite being widely used to study the first hyperpolarizabilities of individual chromophores, to the best of our knowledge, the TSM has not been previously applied to disordered chromophore aggregates or bulk molecular solids. In itself, the TSM does not provide a computational advantage over the CPHF method. However, the computational cost of first hyperpolarizability calculations based on the TSM can be greatly reduced by employing the molecular exciton approximation (MEA). A Hamiltonian constructed within this approximation allows modeling the excitonic interactions in chromophore aggregates, whether disordered or crystalline.^{85,86} The excitonic Hamiltonian can be parametrized on the basis of excitation energies and transition densities computed using TDDFT for single chromophores: an embarrassingly parallelizable task. Performing these calculations in the presence of partial atomic charges that represent the electrostatic environment of the chromophores accounts for interchromophore polarization.⁸⁷ Because the excitonic Hamiltonian uses only one or a small number of basis states per chromophore, it becomes possible to perform calculations on disordered molecular systems with up to $\sim 10^4$ chromophores (rather than atomic basis functions).

The molecular exciton approximation is commonly invoked to explain the optical properties of chromophore aggregates.^{88,89} For instance, we have recently shown that linear absorption spectra of OEO chromophore aggregates computed within this approximation compare well with spectra computed with all-electron methods such as TDDFT.⁸⁷ The method is convenient for modeling exciton-transfer dynamics between chromophores.⁹⁰ The molecular exciton approximation was also used by Suponitsky and Masunov to qualitatively explain trends observed for the first hyperpolarizability of chromophore pairs.⁵⁰ However, to the best of our knowledge, the molecular exciton approximation has never been used for calculating the first hyperpolarizability of multichromophore systems.

In this paper, we compare the values of the first hyperpolarizability calculated using CPHF and the TSM for individual YLD124 chromophores. We then demonstrate how the derivation of the TSM expression for the static first hyperpolarizability can be extended to multichromophore aggregates. We further show that the molecular exciton approximation to the TSM makes it possible to compute first hyperpolarizabilities of large chromophore aggregates while accounting for excitonic interactions between chromophores. We use the CPHF method, the TSM, and various approximate methods that are based on them to calculate the first hyperpolarizability of disordered chromophore aggregates selected from a snapshot in a coarse-grained Monte Carlo simulation.⁹¹ (Two representative 4-chromophore aggregates of YLD124 are shown in Figure 2). We explore the accuracy of the approximations made in each of the methods considered and describe the effects of interchromophore excitonic interactions and mutual electrostatic polarization on the first hyperpolarizability of chromophore aggregates. We also analyze the effects of relative orientation in pairs of identical YLD124 chromophores on the total first hyperpolarizability of the pair. Finally, we use the molecular exciton approximation to analytically calculate the first hyperpolarizability of a one-dimensional periodic array of chromophores and predict the

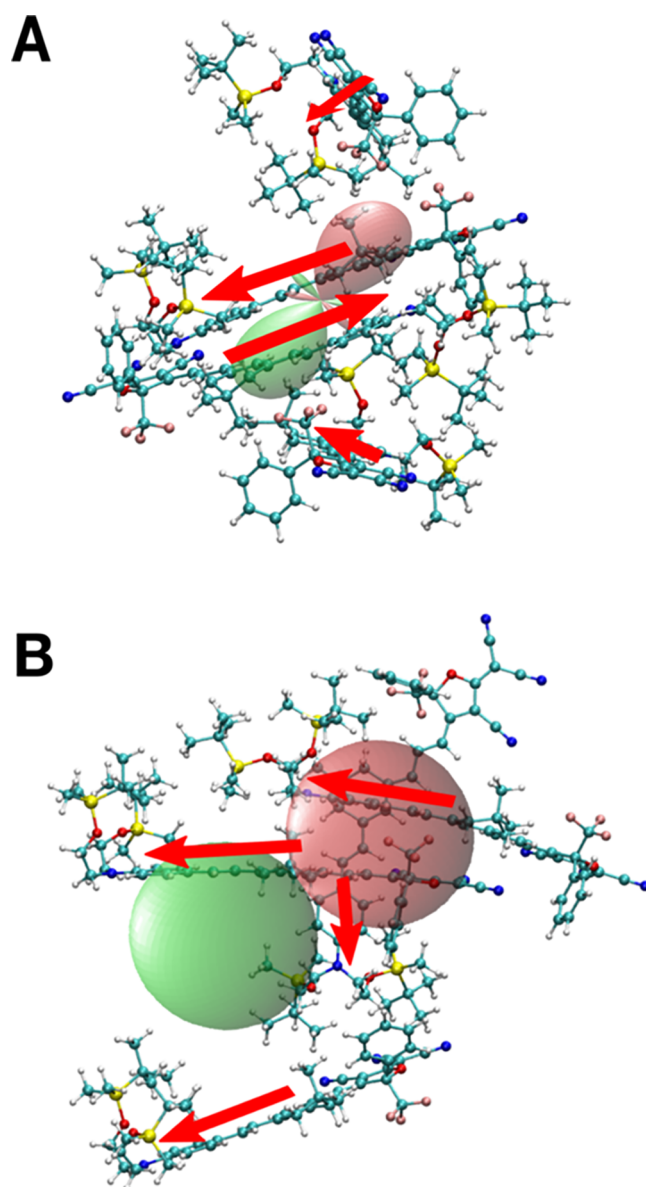


Figure 2. Structures of two 4-chromophore aggregates (tetramers) of YLD124 studied in this paper. Carbon atoms are cyan, oxygen atoms are red, nitrogen atoms are blue, silicon atoms are yellow, and fluorine atoms are pink. The dipole moments of the individual chromophores are represented by arrows. The first hyperpolarizability tensor surface computed using CPHF is overlaid on the aggregate, aligned with the direction of the dipole moment vector. The structure of the aggregate with the smallest computed first hyperpolarizability consists of chromophores with dipole moments predominantly antialigned (A), whereas the structure for the aggregate with the largest computed first hyperpolarizability consists of chromophores with dipole moments predominantly aligned (B).

orientations of chromophores that enhance and decrease bulk electro-optic response.

2. METHODS

2.1. Definition of the First Hyperpolarizability.

Integrating the first-order energy correction within perturbation theory, the electronic energy of a molecular system in a static uniform electric field \vec{F} can be expressed within the dipole approximation as

$$E(\vec{F}) = E(0) - \sum_{\eta} \mu_{\eta}(\vec{F}) F_{\eta} \quad (1)$$

where $\vec{\mu}$ is the dipole moment of the system, $\eta \in \{x, y, z\}$, and the summation is over all possible values. This expression describes the contribution of the dipole term in the multipole expansion of the molecular system's electron density to the total energy of the system in an external electric field \vec{F} and neglects all higher-order terms. The minus sign indicates that application of an electric field lowers the energy. The components of the field-dependent dipole moment can be expanded into a Taylor series with respect to the electric field components

$$\mu_{\eta}(\vec{F}) = \mu_{\eta}(0) + \sum_{\sigma} \alpha_{\eta\sigma} F_{\sigma} + \frac{1}{2} \sum_{\sigma} \sum_{\tau} \beta_{\eta\sigma\tau} F_{\sigma} F_{\tau} + O(F^3) \quad (2)$$

where $\vec{\mu}(0)$ is the permanent dipole moment, $\vec{\alpha}$ is the linear polarizability, $\vec{\beta}$ is the first hyperpolarizability, $\eta, \sigma, \tau \in \{x, y, z\}$, and $O(F^3)$ represents higher-order terms with respect to the electric field, \vec{F} , starting with the term that contains the molecular second hyperpolarizability, γ . Introducing eq 2 into eq 1 and neglecting higher-order terms, we obtain

$$E(F) = E(0) - \sum_{\eta} \mu_{\eta}(0) F_{\eta} - \sum_{\eta} \sum_{\sigma} \alpha_{\eta\sigma} F_{\eta} F_{\sigma} - \frac{1}{2} \sum_{\eta} \sum_{\sigma} \sum_{\tau} \beta_{\eta\sigma\tau} F_{\eta} F_{\sigma} F_{\tau} \quad (3)$$

Taking the first derivative of the electronic energy given by eq 3 with respect to F_{κ} at $\vec{F} = 0$, we obtain the following expression for the components of the permanent ground-state dipole moment

$$\left. \frac{\partial E}{\partial F_{\kappa}} \right|_{\vec{F}=0} = - \sum_{\eta} \mu_{\eta}(0) \frac{\partial F_{\eta}}{\partial F_{\kappa}} = - \sum_{\eta} \mu_{\eta}(0) \delta_{\kappa\eta} = -\mu_{\kappa}(0) \quad (4)$$

where we have used the independence of the electric field components $\frac{\partial F_{\eta}}{\partial F_{\kappa}} = \delta_{\kappa\eta}$ and $\delta_{\kappa\eta}$ is the Kronecker delta. Similarly, taking the second derivative of eq 3 with respect to F_{κ} and F_{λ} at $\vec{F} = 0$ gives the components of the polarizability

$$\left. \frac{\partial^2 E}{\partial F_{\kappa} \partial F_{\lambda}} \right|_{\vec{F}=0} = -(\alpha_{\lambda\kappa} + \alpha_{\kappa\lambda}) \quad (5)$$

and taking the third derivative of eq 3 with respect to F_{κ} , F_{λ} , and F_{ν} at $\vec{F} = 0$ gives the components of the first hyperpolarizability

$$\left. \frac{\partial^3 E}{\partial F_{\kappa} \partial F_{\lambda} \partial F_{\nu}} \right|_{\vec{F}=0} = -\frac{1}{2} (\beta_{\nu\lambda\kappa} + \beta_{\nu\kappa\lambda} + \beta_{\lambda\nu\kappa} + \beta_{\lambda\kappa\nu} + \beta_{\kappa\nu\lambda} + \beta_{\kappa\lambda\nu}) \quad (6)$$

For the static first hyperpolarizability, the order of differentiation with respect to the electric field components is irrelevant. Therefore, the summands in parentheses in eqs 5 and 6 should all be equal. We then obtain the following expression for the components of the first hyperpolarizability tensor

$$\beta_{\kappa\lambda\nu} = -\frac{1}{3} \frac{\partial^3 E}{\partial F_{\kappa} \partial F_{\lambda} \partial F_{\nu}} \Big|_{\vec{F}=0} \quad (7)$$

The expression for the first hyperpolarizability given by eq 7 can be evaluated using the CPHF method.^{57–61}

The first hyperpolarizability of molecular systems can be approximated using a TSM. Oudar and Chemla originally derived both the static and frequency-dependent TSM for single donor–acceptor chromophores,^{63,64} but in the Supporting Information we show that the TSM derivation of the static first hyperpolarizability can be extended to more complex systems, such as chromophore aggregates, by using an alternative basis (see Figure S1). For the components of the static first hyperpolarizability tensor, the two-state model expression is

$$\beta_{\kappa\lambda\nu} = \frac{2\mu_{\kappa}^{|\Psi_{-}\rangle \rightarrow |\Psi_{+}\rangle} \mu_{\lambda}^{|\Psi_{-}\rangle \rightarrow |\Psi_{+}\rangle} (\mu_{\nu}^{|\Psi_{+}\rangle} - \mu_{\nu}^{|\Psi_{-}\rangle})}{(E_{+} - E_{-})^2} \quad (8)$$

where $\mu^{|\Psi_{-}\rangle \rightarrow |\Psi_{+}\rangle}$ is the transition dipole moment between the ground state $|\Psi_{-}\rangle$ and an excited state $|\Psi_{+}\rangle$ of the aggregate, $\mu^{|\Psi_{+}\rangle}$ and $\mu^{|\Psi_{-}\rangle}$ are the excited- and ground-state dipole moments of the aggregate, respectively, and $(E_{+} - E_{-})$ is the ground-to-excited-state excitation energy.

Equation 8 expresses the static first hyperpolarizability of a two-level system. In this paper, we use it to calculate contributions to the first hyperpolarizability due to the interaction between the ground state of a chromophore aggregate and an individual excited state. The total first hyperpolarizability of the aggregate is assumed to be the sum of these contributions over all excited states. We neglect any interactions between excited states of the aggregate, either directly or via the ground state. This approximation is reasonable in the limit of weak couplings between chromophores in the aggregate.

2.2. Molecular Exciton Approximation to the Two-State Model. We have previously evaluated the performance of the molecular exciton approximation for calculations of the linear absorption spectra of chromophore aggregates.⁸⁷ The same approximation can readily be applied to calculations of the parameters that enter the two-state model expression for the first hyperpolarizability.

The tight-binding molecular exciton Hamiltonian for the single-excitation manifold of an aggregate that consists of N chromophores is of the form^{85,86}

$$\hat{H} = \sum_{i=1}^N \omega_i \hat{a}_i^{\dagger} \hat{a}_i + \sum_{i=1}^N \sum_{j=1}^{i-1} J_{ij} (\hat{a}_i^{\dagger} \hat{a}_j + \hat{a}_i \hat{a}_j^{\dagger}) \quad (9)$$

where ω_i is the excitation energy of the i th chromophore, J_{ij} is the excitonic coupling between the i th and the j th chromophores, and \hat{a}_i^{\dagger} and \hat{a}_i are the creation and annihilation operators, respectively, for an excitation on the i th chromophore: $\hat{a}_i^{\dagger} |0\rangle_i = |1\rangle_i$, $\hat{a}_i^{\dagger} |1\rangle_i = 0$ and $\hat{a}_i |1\rangle_i = |0\rangle_i$, $\hat{a}_i |0\rangle_i = 0$, where $|0\rangle_i$ and $|1\rangle_i$ are the ground and excited states of the i th chromophore. The Hamiltonian given by eq 9 can be parametrized using ab initio calculations on single chromophores, as discussed in ref 87.

In the limit of weak interchromophore interactions in the ground state, the ground state of an aggregate that consists of N chromophores can be approximated by

$$|\emptyset\rangle = \otimes_{i=1}^N |0\rangle_i \equiv |0\rangle_1 \otimes \dots \otimes |0\rangle_N \quad (10)$$

Assuming that there is only one excited state $|1\rangle_i$ that is localized on the i th chromophore, that chromophores in the excited state interact weakly with chromophores in the ground state, and that the spatial density of excitations in the material is low, the excited states of the aggregate can be expressed as

$$|\Psi_k\rangle = \sum_{j=1}^N c_j^k |\Phi_j\rangle \quad (11)$$

with generally complex coefficients c_j^k in the Frenkel exciton basis⁹²

$$|\Phi_j\rangle = \otimes_{i=1}^N |\delta_{ij}\rangle, \quad j = 1, \dots, N \quad (12)$$

where δ_{ij} is the Kronecker delta. Thus, in the state $|\Phi_j\rangle$, the j th chromophore is in its excited state $|1\rangle_j$ and all other chromophores are in their ground states $|0\rangle_{i \neq j}$.

The components of the first hyperpolarizability tensor predicted by the two-state model are given by eq 8. Within the molecular exciton model, the lowest excitation energy is simply the lowest eigenvalue of the Hamiltonian, given by eq 9. The ground state $\vec{\mu}^{g(\Psi_-)} = \vec{\mu}^{g(\emptyset)}$, the excited state $\vec{\mu}^{e(\Psi_+)} = \vec{\mu}^{e(\Psi_k)}$, and the ground-to-excited-state transition $\vec{\mu}^{g(\Psi_-) \rightarrow e(\Psi_+)} = \vec{\mu}^{g(\emptyset) \rightarrow e(\Psi_k)}$ dipole moments for a chromophore aggregate can be expressed in terms of the ground state $\vec{\mu}_i^g$, excited state $\vec{\mu}_i^e$, and ground-to-excited-state transition $\vec{\mu}_i^{ge}$ dipole moments of individual chromophores, $i = 1, \dots, N$. The calculations are performed for all $|\Psi_k\rangle$, $k = 1, \dots, N$.

Equation 10 represents the ground state of N noninteracting chromophores in their ground states. Therefore, the ground-state dipole moment for this system is simply a vector sum of the ground-state dipole moments of individual chromophores

$$\vec{\mu}^{g(\emptyset)} = \sum_{i=1}^N \vec{\mu}_i^g \quad (13)$$

Similarly, the permanent dipole moments of the Frenkel exciton basis states $|\Phi_j\rangle$, given by eq 12, are

$$\vec{\mu}^{g(\Phi_j)} = \vec{\mu}_j^e + \sum_{i \neq j} \vec{\mu}_i^g \quad (14)$$

where $j = 1, \dots, N$. For an arbitrary state $|\Psi_k\rangle$ in the single-excitation manifold of the chromophore aggregate, the permanent dipole moment is the sum of dipole moments of the Frenkel exciton basis states $|\Phi_j\rangle$ given by eq 14, weighted by the contributions of these basis states to state $|\Psi_k\rangle$, i.e., by the squares of the absolute values of expansion coefficients c_j^k in eq 11

$$\vec{\mu}^{g(\Psi_k)} = \sum_{j=1}^N |c_j^k|^2 \vec{\mu}^{g(\Phi_j)} \quad (15)$$

To obtain the transition dipole moment of a chromophore aggregate, one must evaluate the matrix element

$$\vec{\mu}^{g(\emptyset) \rightarrow e(\Psi_k)} = \langle \Psi_k | \hat{\mu}^{\rightarrow ge} | \emptyset \rangle \quad (16)$$

with the transition dipole operator

$$\hat{\mu}^{\rightarrow ge} = \sum_{i=1}^N \vec{\mu}_i^{ge} (\hat{a}_i^\dagger + \hat{a}_i) \quad (17)$$

If multiple excitations are not allowed within a chromophore aggregate, then introducing eqs 17 and 11 into eq 16 yields

$$\begin{aligned} \vec{\mu}^{g(\emptyset) \rightarrow e(\Psi_k)} &= \langle \Psi_k | \hat{\mu}^{\rightarrow ge} | \emptyset \rangle = \sum_{i=1}^N \vec{\mu}_i^{ge} \langle \Psi_k | (\hat{a}_i^\dagger + \hat{a}_i) | \emptyset \rangle = \sum_{i=1}^N \vec{\mu}_i^{ge} \langle \Psi_k | \Phi_i \rangle \\ &= \sum_{i=1}^N \vec{\mu}_i^{ge} \sum_{j=1}^N (c_j^k)^* \langle \Phi_j | \Phi_i \rangle = \sum_{i=1}^N \vec{\mu}_i^{ge} \sum_{j=1}^N (c_j^k)^* \delta_{ij} = \sum_{i=1}^N (c_i^k)^* \vec{\mu}_i^{ge} \end{aligned} \quad (18)$$

The lowest eigenvalue of the Hamiltonian given by eq 9 that can be obtained by diagonalizing the Hamiltonian, as well as the ground state, excited state, and transition dipole moments calculated using eqs 13–15 and 18 are all of the parameters required to calculate the first hyperpolarizability according to eq 8.

2.3. Computational Details. The Gaussian 09 quantum chemistry package⁹³ was used for all ab initio calculations. Calculations were performed both on the optimized geometry of a single YLD124 chromophore and on disordered chromophores obtained from the same snapshot in a course-grained Monte Carlo simulation⁹¹ that was used in ref 87. Geometry optimization of YLD124 was performed in vacuum using the B3LYP density functional and the 6-31G* basis set.^{94,95} All electronic structure calculations of the energies, dipole moments (ground state, excited state, and transition), and first hyperpolarizabilities used the ω B97X long-range corrected density functional⁹⁶ and the 6-31G* basis set. This basis set is not large enough to predict properties converged with respect to the size of the basis set. However, we herein provide a comparison of theoretical methods and the all-electron CPHF calculations would not be feasible for the larger aggregates using a larger basis set. Direct calculation of the first hyperpolarizability was performed using the CPHF method.

Excitonic Hamiltonians were parametrized following the procedure described in ref 87. The excitation energies of individual chromophores were calculated using ω B97X/6-31G*. Excitonic couplings were calculated using the transition density cube method that captures the Coulombic contribution to the interchromophore couplings J_{ij} , neglecting the effects of electron exchange and correlation.⁹⁷ Transition density matrices from Gaussian calculations were converted to average transition densities for small cubic spatial regions that spanned the rectangular volume encompassing each chromophore using the Multiwfn program⁹⁸ with a coarse grid (the “1” setting). The couplings were then expressed as⁹⁷

$$J_{ij} = \frac{1}{2} \sum_m \sum_l \frac{M_i^m M_j^l}{4\pi\epsilon_0 r_{ml}^{ij}} \quad (19)$$

where M_i^m and M_j^l are the average transition densities for the m th cubic volume for the i th chromophore and the l th cubic volume for the j th chromophore, r_{ml}^{ij} is the distance between the centers of these cubic volumes, the summation runs over all cubic volumes that the spatial regions of both chromophores are fragmented into, ϵ_0 is the electrical constant, and the factor $\frac{1}{2}$ is necessary to prevent double-counting interactions.

Sample input and output TDDFT and CPHF data for the optimized geometry of YLD124 are provided in the [Supporting Information](#). To account for polarization of the electron density on a chromophore by the surrounding chromophores, we represented this electrostatic environment by the CHELPG partial atomic charges.⁹⁹ In ref 87, we found that the polarization of the chromophores by the surrounding environment improved the agreement between the molecular exciton

model and the TDDFT aggregate calculations for the aggregates of highly dipolar YLD124 chromophores. It is unclear if inclusion of charges would be similarly beneficial for less dipolar chromophores, such as the centrosymmetric systems of interest for their large second hyperpolarizability. In this study, the charges were calculated for individual chromophores at the ω B97X/6-31G* level of theory, then included as fixed point charges in the electronic structure calculations for the chromophore of interest. Calculations that accounted for electrostatic polarization are denoted in this paper by the label “ch” appended to the method name.

For the simulation of disordered aggregates, structures of 25 pairs of chromophores (“dimers”), 25 aggregates of 4 chromophores (“tetramers”), and 25 aggregates of 10 chromophores (“decamers”) were selected from a single snapshot of a coarse-grained Monte Carlo simulation⁹¹ of a disordered solid consisting of YLD124 chromophores using the same procedure as that in ref 87. The coarse-grained simulation was performed with 108 chromophores in the cubic unit cell, using periodic boundary conditions, at 1 atm and 300 K.

For many push–pull molecules, the dominant component of the first hyperpolarizability tensor, β , is its projection onto the molecule’s transition dipole moment that is usually aligned with the ground-state dipole moment and is often oriented along the z -axis. In this case, the electro-optic response of the molecule is maximized when the external electric field is also applied along the z -axis. The electro-optic response is then determined by the β_{zzz} component of the first hyperpolarizability tensor. Consequently, only this component is often reported. However, for the disordered aggregates studied in this paper, the transition dipole moments of individual chromophores are not aligned and no single component of β dominates the electro-optic response. Therefore, for both CPHF and TSM results, we report the magnitude of the first hyperpolarizability β computed as

$$\beta = \sqrt{\beta_x^2 + \beta_y^2 + \beta_z^2} \quad (20)$$

where the i th component of β is given by

$$\beta_i = \beta_{iii} + \sum_{j \neq i} \frac{1}{3} (\beta_{ijj} + \beta_{jjj} + \beta_{jji}) \quad (21)$$

Note that to obtain the magnitude of β , we calculate all components of the first hyperpolarizability tensor. These individual components can be used to investigate the dependence of the electro-optic response of multichromophore systems on their orientation relative to the applied electric field. However, this investigation is beyond the scope of the current work. We report the first hyperpolarizability in atomic units (au). The conversion factor from au to the more commonly used electrostatic units (esu) is 1 au = 8.639×10^{-33} esu.

To plot the tensor surfaces displayed in Figure 2, the WinTensor program¹⁰⁰ was used. Plotting tensor surfaces to visualize the magnitude and direction of optical properties of molecules has been discussed by Simpson and co-workers.^{101,102}

2.4. Summary of Methods for Calculating Hyperpolarizability. Computational cost makes ab initio calculations using the recommended long-range corrected hybrid density functionals practical only for relatively small systems that can be adequately described with up to $\sim 10^4$ atomic basis

functions (e.g., aggregates of 4–5 YLD124 chromophores with the 6-31G* basis set). For such systems, the first hyperpolarizability can be calculated directly using the CPHF method. This method includes the full response of the electron density to the applied field and is in principle equivalent to summing over all excited states of the system. We will refer to it as CPHF-full.

Calculating the first hyperpolarizability of larger chromophore aggregates or of bulk molecular materials requires a different approach. A straightforward way to accomplish this task is by summation of the first hyperpolarizability tensors of individual chromophores that can be rigorously calculated using the CPHF method. We will refer to this method as CPHF-sum. This calculation is embarrassingly parallelizable, as it only requires finding the first hyperpolarizabilities of individual chromophores in the aggregate. It can be further simplified if all chromophores in an aggregate are replaced by chromophores in their optimized geometries, with their ground-state dipole moments oriented in the same way as those for the original chromophores, as has been done in ref 56. In this case, a CPHF first hyperpolarizability calculation need only be performed once for the optimized geometry, with subsequent rotation of the first hyperpolarizability tensor. We will refer to this method as CPHF-sum/opt.

Summing over the first hyperpolarizabilities of individual chromophores neglects excitonic interactions between chromophores. However, interchromophore polarization can be partially accounted for by calculating the first hyperpolarizabilities of individual chromophores in the presence of the partial atomic charges of surrounding chromophores. We will refer to this method as CPHF-sum/ch.

First hyperpolarizabilities of chromophore aggregates can also be approximately calculated using the TSM given by eq 8. This expression involves parameters of the entire aggregate (the ground- and excited-state dipole moments, the transition dipole moment between the ground and excited state, and the excitation energy). For small aggregates, it is possible to obtain these parameters directly from electronic structure calculations on the entire aggregate. We will refer to this method as TSM-full.

TSM-full has scaling similar to CPHF-full, despite being a less rigorous method. Similar to CPHF-sum, it is possible to approximately calculate first hyperpolarizabilities of large chromophore aggregates by summing over first hyperpolarizabilities of individual chromophores calculated using the TSM. We will refer to this method as TSM-sum.

A more rigorous approach than TSM-sum to calculating first hyperpolarizabilities of large aggregates uses the molecular exciton approximation to the TSM to account for excitonic interactions between chromophores. In this approach, the parameters that enter the TSM expression given by eq 8, are expressed in terms of the parameters of individual chromophores using eqs 13–15 and 18. We will refer to the method for calculating the first hyperpolarizability of chromophore aggregates that uses this parametrization of the TSM as TSM-MEA. If the polarization of the electronic density on individual chromophores by their molecular environment is additionally accounted for by performing ab initio calculations on each chromophore in the presence of the atomic point charges on surrounding chromophores, we will refer to this method as TSM-MEA/ch. Because only ab initio calculations on individual chromophores are necessary in the TSM-MEA and TSM-MEA/ch methods, these methods are

Table 1. Methods for Calculating the First Hyperpolarizability of Chromophore Aggregates

method name	description
CPHF-full	all-electron CPHF calculation on the entire chromophore aggregate
CPHF-sum	summation over first hyperpolarizabilities of individual chromophores calculated using the CPHF method
CPHF-sum/ch	CPHF-sum with first hyperpolarizabilities of individual chromophores calculated in the presence of atomic point charges of the surrounding chromophores
CPHF-sum/opt	CPHF-sum for an aggregate where each chromophore is replaced by a chromophore in the optimized geometry with the ground-state dipole moment aligned in the direction same as that for the original chromophore
TSM-full	first hyperpolarizability calculated using the TSM, in eq 8, with the parameters entering the model found from all-electron calculations on the entire chromophore aggregate
TSM-sum	summation over first hyperpolarizabilities of individual chromophores calculated using the TSM
TSM-MEA	first hyperpolarizability calculated using the TSM with the parameters entering the model calculated within the molecular exciton approximation
TSM-MEA/ch	TSM-MEA with the parameters of individual chromophores calculated in the presence of atomic point charges of the surrounding chromophores

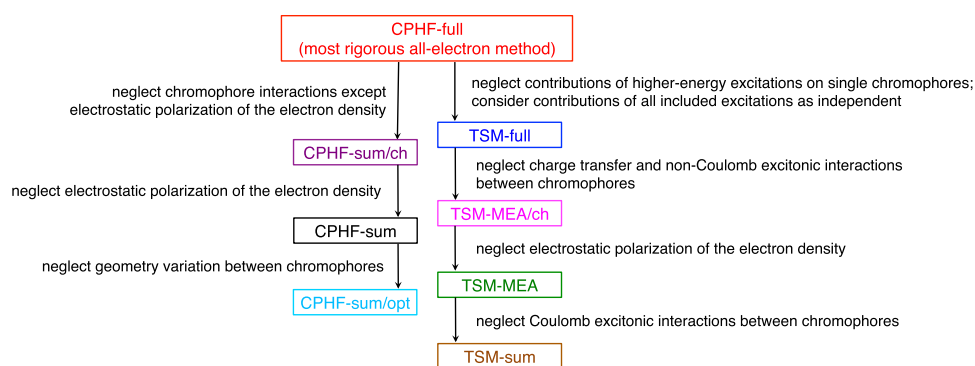


Figure 3. Approximations made in the methods for calculating the first hyperpolarizability of chromophore aggregates. The color-coding for methods that is introduced in this figure is used throughout the manuscript.

embarrassingly parallelizable. The molecular exciton Hamiltonian, eq 9, uses a single basis state per chromophore; therefore, the TSM-MEA or TSM-MEA/ch methods allow calculations on systems with up to $\sim 10^4$ chromophores (rather than atomic basis functions).

Table 1 summarizes the methods for calculating the first hyperpolarizability of chromophore aggregates that are discussed in this paper. Figure 3 illustrates the approximations made in each of these methods. To elucidate the effects of higher-energy excited states, excitonic interactions between chromophores, and electrostatic polarization of the electron density of individual chromophores on the aggregate's first hyperpolarizability, we compare the values calculated using these various methods.

3. RESULTS AND DISCUSSION

3.1. Approximating First Hyperpolarizabilities of Aggregates by a Sum of First Hyperpolarizabilities of Constituent Chromophores Calculated Using CPHF. For chromophore aggregates, a computationally affordable approach to computing the first hyperpolarizability is to perform only a single CPHF calculation on an optimized chromophore, then to use this first hyperpolarizability tensor for all chromophores in the aggregate, ignoring changes in the first hyperpolarizability due to changes in chromophore geometry and interchromophore interactions (CPHF-sum/opt). This method and a similar technique where the value of the first hyperpolarizability of a single chromophore is simply scaled by the order parameter has been used in previous work⁵⁶ to give a rough estimate of the first hyperpolarizability of chromophore aggregates. However, Figure 4 shows that the CPHF-sum/opt method performs rather poorly compared with the CPHF-full

benchmark results, with errors and standard deviations of $(0.022 \pm 0.163) \times 10^6$ au for 25 dimers and $(0.085 \pm 0.243) \times 10^6$ au for 25 tetramers (also see Table 2). For reference, the CPHF-full tensor surface is plotted^{101,102} for the tetramers with the smallest and the largest first hyperpolarizability in Figure 2A,B, respectively.

For the CPHF-sum method that uses the actual geometries of the monomers in the aggregate, the mean error relative to CPHF-full does not change significantly for dimers and reduces by more than a factor of 3 for tetramers compared with the CPHF-sum/opt method. The standard deviation reduces by more than half, to 0.077×10^6 au for dimers and 0.098×10^6 au for tetramers (see Table 2). This result shows that geometric distortions strongly affect the first hyperpolarizability and should be accounted for if at all possible.

The agreement with first hyperpolarizability values calculated using the CPHF-full method can be further improved by accounting for the polarization of the electronic density on the chromophores by their molecular environment using the CPHF-sum/ch method. Including this polarization does not change the mean error relative to CPHF-full significantly but reduces the standard deviation by a factor of more than 1.5 compared with the CPHF-sum method (to 0.049×10^6 au for dimers and 0.060×10^6 au for tetramers, see Table 2).

The positive values of the mean error relative to CPHF-full for CPHF-sum/opt, CPHF-sum, and CPHF-sum/ch calculations indicate that all three approximate methods systematically slightly overestimate the first hyperpolarizability of chromophore aggregates. This overestimation is similar for dimers and tetramers for the CPHF-sum and CPHF-sum/ch methods, whereas it is larger for tetramers than for dimers for the CPHF-sum/opt method. The error is likely related to the

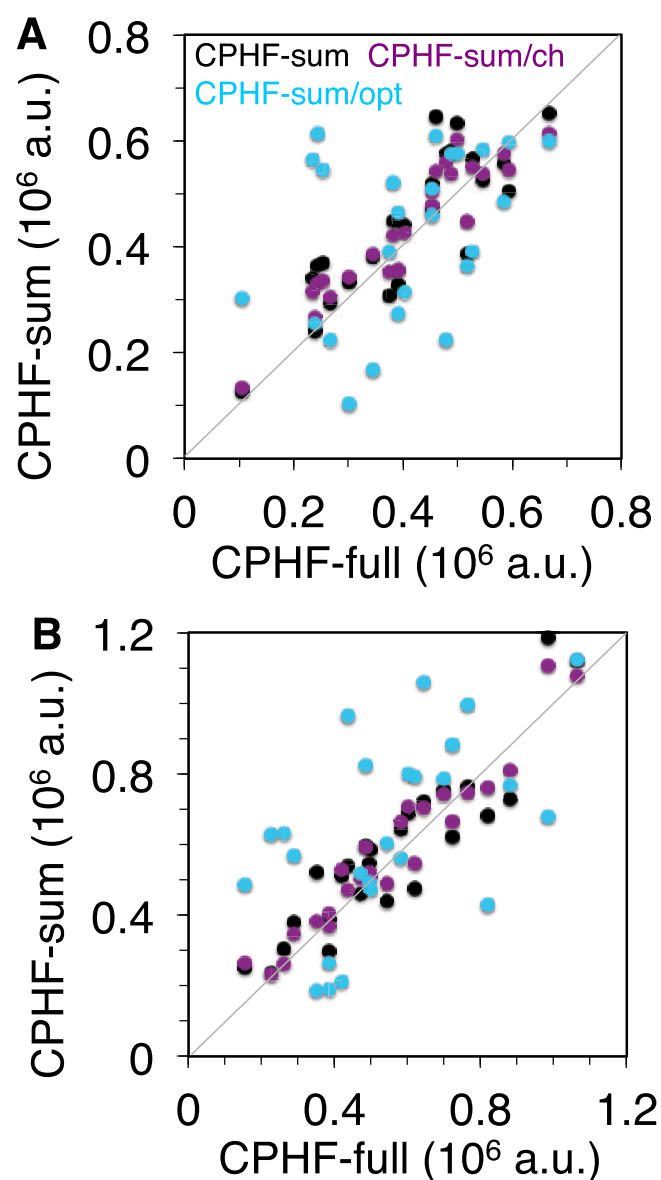


Figure 4. Comparison of the first hyperpolarizabilities calculated using the CPHF-sum (black), the CPHF-sum/ch (violet), and the CPHF-sum/opt (light blue) methods to values calculated using the CPHF-full method for 25 dimers (A) and 25 tetramers (B) of YLD124 chromophores selected from a Monte Carlo snapshot. The dotted line denotes perfect agreement.

neglect of excitonic interactions in the CPHF-sum, CPHF-sum/ch, and CPHF-sum/opt methods, suggesting that excitonic interactions are likely to decrease the value of the first hyperpolarizability for these systems. In Section 3.4, we will see that inclusion of excitonic interactions lowers the mean value of the first hyperpolarizability for the disordered chromophore aggregates considered here. In Section 3.5, we will explore how excitonic interactions affect the first hyperpolarizability for various relative orientations of chromophores.

The covariance between the deviation of the aggregate's first hyperpolarizability from the CPHF-full value and the magnitude of the CPHF-full first hyperpolarizability is very small for all three approximate methods considered. Therefore, the absolute errors with respect to CPHF-full for the first hyperpolarizability values calculated using these methods are

Table 2. Mean Error $\langle \beta - \beta_{\text{CPHF-full}} \rangle$ for the First Hyperpolarizabilities Calculated Using the TSM-Full, TSM-Sum, TSM-MEA, TSM-MEA/Ch, CPHF-Sum, CPHF-Sum/Ch, and CPHF-Sum/Opt Methods relative to the Values Calculated Using the CPHF-Full Method, the Standard Deviations $\sigma_{\beta - \beta_{\text{CPHF-full}}}$ for These Errors, and the Covariance $\text{cov}(\beta - \beta_{\text{CPHF-full}}, \beta_{\text{CPHF-full}})$ of the Mean Error for the First Hyperpolarizability with the Value of the First Hyperpolarizability Calculated Using the CPHF-Full Method

	method	mean error	σ	cov
dimers	TSM-full	-0.076	0.057	9.3×10^{-4}
	TSM-sum	+0.055	0.103	-2.1×10^{-3}
	TSM-MEA	-0.043	0.110	-1.8×10^{-2}
	TSM-MEA/ch	-0.046	0.099	-1.7×10^{-3}
	CPHF-sum	+0.028	0.077	-2.7×10^{-3}
	CPHF-sum/ch	+0.025	0.049	-2.8×10^{-3}
tetramers	CPHF-sum/opt	+0.020	0.163	-9.8×10^{-3}
	TSM-full	-0.052	0.142	-1.7×10^{-2}
	TSM-sum	+0.058	0.115	-3.4×10^{-4}
	TSM-MEA	-0.062	0.173	-1.8×10^{-2}
	TSM-MEA/ch	-0.063	0.139	7.1×10^{-3}
	CPHF-sum	+0.026	0.098	-4.4×10^{-3}
CPHF-sum/ch	+0.025	0.060	-3.0×10^{-3}	
CPHF-sum/opt	+0.085	0.243	-2.0×10^{-3}	

independent of the magnitude of the first hyperpolarizability. The relative errors are, consequently, larger for chromophore aggregates with smaller first hyperpolarizabilities.

Figure 4 and Table 2 show that for the dimers and tetramers, the accuracy of the first hyperpolarizability calculated using the CPHF-sum/ch method relative to the CPHF-full method provides the smallest standard deviation of the approximate methods considered.

3.2. Effect of Higher-Energy Excited States on the First Hyperpolarizability of Single YLD124 Chromophores. Methods that approximate the first hyperpolarizability of a chromophore aggregate as the sum of the first hyperpolarizabilities of individual chromophores calculated using CPHF (CPHF-sum/ch, CPHF-sum, and CPHF-sum/opt) account for all states of individual chromophores but neglect the possibility of exciton delocalization between chromophores. Excitonic interactions that lead to such delocalization are included in the computationally efficient TSM-MEA and TSM-MEA/ch methods. However, all methods based on the TSM neglect contributions of higher-energy excited states of individual chromophores on the first hyperpolarizability (see Figure 3). To estimate the error that this approximation introduces, we compare the values of the first hyperpolarizability, β , calculated using the CPHF method and the TSM expression, eq 8, for the optimized geometry of the YLD124 chromophore (unfilled triangle) and for 57 individual YLD124 chromophores from the Monte Carlo snapshot (solid circles). This comparison is shown in Figure 5. The structure of the chromophores leads to 18% variation in the value of β , ranging from 0.316 to 0.371×10^6 au when calculated using the CPHF method.

The TSM expression systematically overestimates the first hyperpolarizability compared to the CPHF value by $(0.024 \pm 0.008) \times 10^6$ au. There is no correlation between the first hyperpolarizability value and the amount by which it is overestimated (covariance -3.0×10^{-5}). Therefore, the

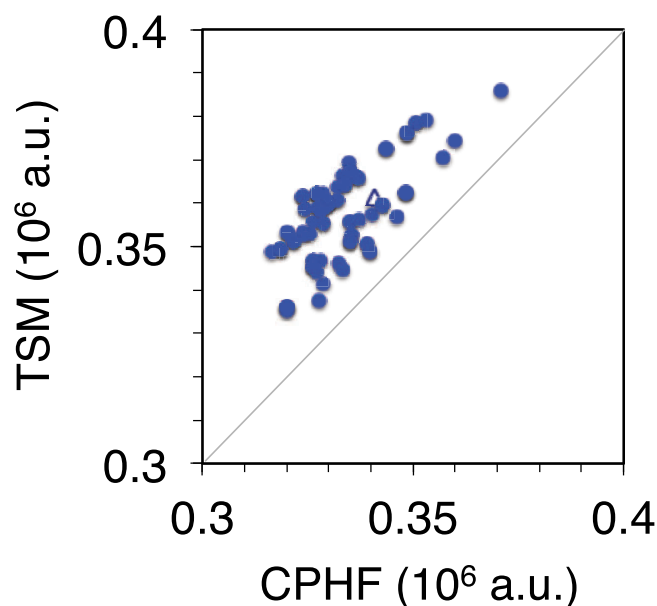


Figure 5. Comparison of the first hyperpolarizabilities calculated using the coupled-perturbed Hartree–Fock (CPHF) method and the two-state model (TSM) for 57 YLD124 chromophores from a Monte Carlo snapshot (solid circles) and for the B3LYP/6-31G* optimized YLD124 geometry (unfilled triangle). The gray line denotes perfect agreement.

relative error is smaller for larger first hyperpolarizability values; for all values it does not exceed 7%. The systematic overestimation of β by the TSM suggests that contributions to β by high-lying excited states are opposite in sign to the contributions to β by the bright lowest-energy state. The agreement between the TSM and CPHF values is similar to that found by Paschoal et al.⁸⁰ for a set of OEO chromophores.

3.3. Effect of Higher-Energy Excited States of Single Chromophores on the First Hyperpolarizability of Chromophore Aggregates. All states in the band that is formed due to the interaction of the lowest bright excited states of individual chromophores in an aggregate contribute to the aggregate's first hyperpolarizability. The TSM can be used to calculate the contribution of each state in that band, and the total first hyperpolarizability of the aggregate can then be found as a sum of the first hyperpolarizability tensors over all states in the band. Although all excited states in the full-TSM treatment are calculated together within the TDDFT computation and therefore implicit coupling between the states is accounted for within TDDFT, summing the TSM hyperpolarizability tensors as in the TSM-full method assumes that the contributions of all excited states within the band to the first hyperpolarizability of a chromophore aggregate are independent. To test the effect of this assumption on the accuracy of the TSM for chromophore aggregates, we compare the values of the first hyperpolarizability β calculated using the CPHF-full method and the TSM expression, eq 8, parametrized using all-electron TDDFT calculations (TSM-full) for the 25 chromophore dimers and 25 chromophore tetramers selected from the coarse-grained Monte Carlo simulation snapshot.

As with the monomers, a reasonable agreement between the first hyperpolarizability values calculated using the CPHF-full and the TSM-full methods is found for the small chromophore aggregates, as shown in Figure 6. In contrast to the results for

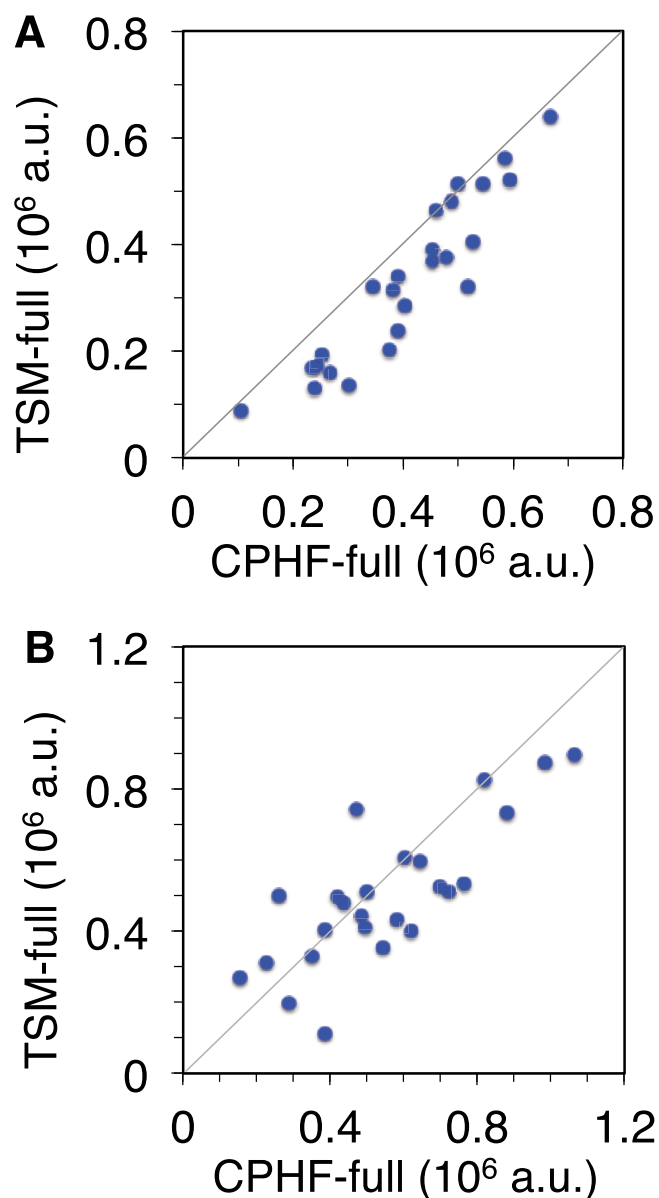


Figure 6. Comparison of the first hyperpolarizabilities calculated using the CPHF-full and TSM-full methods for 25 dimers (A) and 25 tetramers (B) of YLD124 chromophores selected from a Monte Carlo snapshot. The gray line denotes perfect agreement.

the monomers, on average, the TSM-full method underestimates the first hyperpolarizability compared to the CPHF-full value for both dimers and tetramers, by $(-0.076 \pm 0.057) \times 10^6$ au and $(-0.052 \pm 0.142) \times 10^6$ au, respectively. The underestimation of β by the TSM for dimers and tetramers can be rationalized by examining the trend in the CPHF and TSM β values for chromophore dimers rotated from parallel to perpendicular orientations, as shown in Figure S2. Only for parallel dimers is the β value overestimated by the TSM. For a large span of angles between the chromophores, the TSM underestimates β . Because the parallel orientation of a pair of chromophores is energetically unfavorable due to repulsion between their permanent dipole moments, it rarely occurs in chromophore dimers and tetramers.

As in the case of monomers, there is no correlation between the first hyperpolarizability value and the discrepancy between CPHF-full and TSM-full values (covariance 9.3×10^{-4} for

dimers and -1.7×10^{-2} for tetramers). Therefore, the relative error is smaller for larger first hyperpolarizability values. Because the absolute error in the TSM-full first hyperpolarizability with respect to the CPHF-full first hyperpolarizability is uncorrelated with the magnitude of the first hyperpolarizability, the relative errors for aggregates with small first hyperpolarizabilities can be larger than those for monomers.

3.4. Effect of Excitonic Interactions on the First Hyperpolarizabilities of Disordered Chromophore Aggregates. In calculations of the first hyperpolarizability, β , of chromophore aggregates using the computationally efficient TSM-MEA and TSM-MEA/ch methods, errors are due to both the TSM and the molecular exciton approximation (where charge transfer between chromophores is not accounted for and interchromophore polarization is only partially accounted for via the fixed partial atomic charges in the TSM-MEA/ch method). Therefore, the applicability of the TSM-MEA and TSM-MEA/ch methods to calculations of β hinges on two conditions. The first condition is that the TSM-full method reproduces values calculated using the more accurate CPHF-full method. In Sections 3.2 and 3.3, we have seen that the agreement between TSM-full and CPHF-full is reasonable for both monomers and small aggregates of YLD124 chromophores. The second condition is that parameters entering the TSM expression for the first hyperpolarizability, eq 8, that are calculated within the molecular exciton approximation (using the TSM-sum, TSM-MEA, or TSM-MEA/ch methods) agree with those obtained from ab initio calculations on entire aggregates (the TSM-full method).

In this section, we compare the first hyperpolarizability values calculated for the same 25 dimers and 25 tetramers as in Figure 6 using the TSM-sum, TSM-MEA, and TSM-MEA/ch methods to values calculated using the TSM-full and CPHF-full methods. In Section 3.5, we will explicitly consider the accuracy of calculating parameters that enter eq 8 within the molecular exciton approximation for different chromophore arrangements.

To isolate the effect of excitonic interactions from the effects of approximations intrinsic to the TSM, the β values computed by summing up the first hyperpolarizability tensors for individual chromophores (the TSM-sum method) are also compared to those computed using the TSM-full method. These results are shown in Figure 7.

The values of the first hyperpolarizability calculated using the TSM-full and TSM-MEA methods agree well, with errors of $(0.033 \pm 0.081) \times 10^6$ au for dimers and $(-0.009 \pm 0.125) \times 10^6$ au for tetramers. The agreement between the TSM-full and the TSM-MEA/ch methods is even better, with similarly small average errors and reduced standard deviations: $(0.029 \pm 0.055) \times 10^6$ au for dimers and $(-0.011 \pm 0.095) \times 10^6$ au for tetramers. The agreement is not as good for the TSM-sum method, where excitonic interactions are neglected: $(0.131 \pm 0.083) \times 10^6$ au for dimers and $(0.111 \pm 0.160) \times 10^6$ au for tetramers. The larger error and the larger standard deviation suggests that including the excitonic interaction between chromophores can significantly improve the accuracy of the computed first hyperpolarizability. In all cases, there is no correlation between the first hyperpolarizability value and the error in it, with covariances in the interval $(-5.0 \times 10^{-3}, 5.0 \times 10^{-3})$.

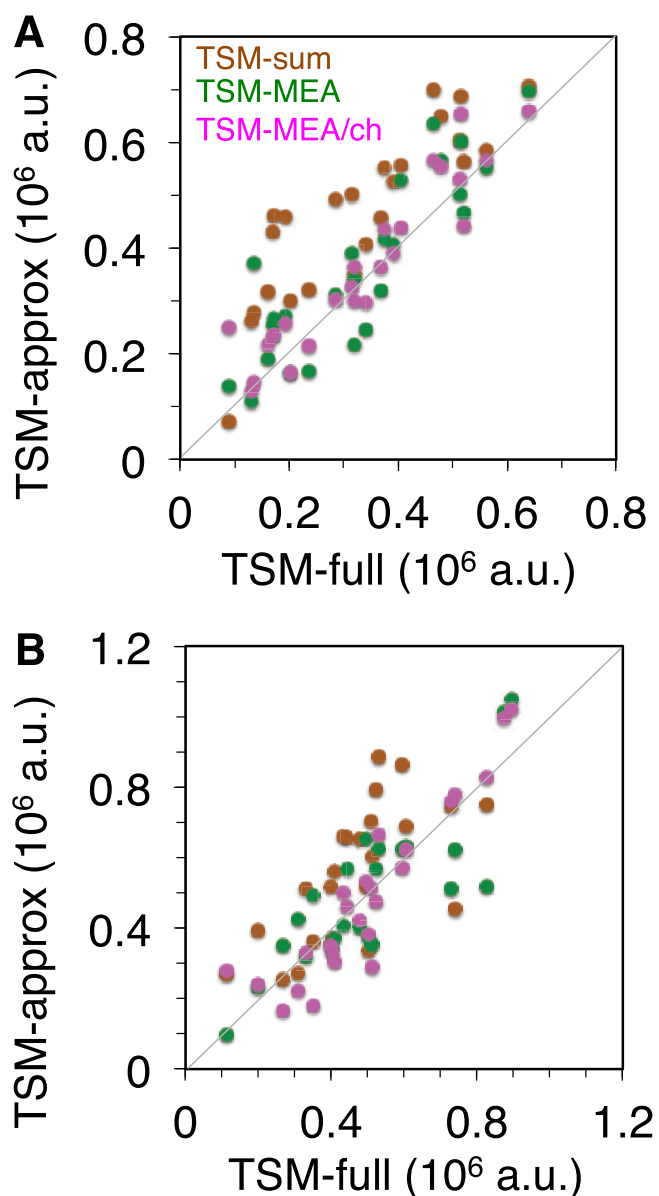


Figure 7. Comparison of the first hyperpolarizabilities calculated using the TSM-MEA (green), the TSM-MEA/ch (magenta), and the TSM-sum (brown) methods to values calculated using the TSM-full method for the same 25 dimers (A) and 25 tetramers (B) as those in Figure 6. The dotted line denotes perfect agreement.

To assess the effect of excitonic interactions on the first hyperpolarizability for larger aggregates, we compare β values calculated using the TSM-MEA and TSM-sum methods for disordered chromophore dimers, tetramers, and decamers selected from a coarse-grained Monte Carlo simulation snapshot (Figure 8). The agreement between the absolute values of the first hyperpolarizability calculated using the two methods gets progressively worse with increasing size of the aggregates. The contribution of excitonic effects to the first hyperpolarizability of the aggregate seems to scale nearly linearly with the number of chromophores in the aggregate. For dimers, including excitonic effects reduces the absolute magnitude of the first hyperpolarizability by $13.6 \pm 10.6\%$ of the value for the optimized YLD124 monomer geometry per chromophore. For tetramers and decamers, the reduction is by 12.3 ± 5.3 and $12.1 \pm 6.9\%$ of the value for the optimized

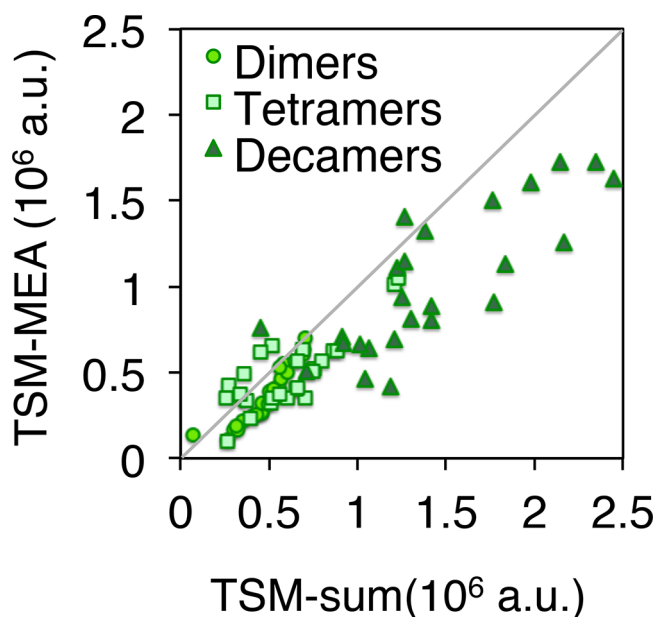


Figure 8. Comparison of the first hyperpolarizability values calculated using the TSM-MEA and TSM-sum methods for 25 dimers (circles), 25 tetramers (squares), and 25 decamers (triangles). The gray line denotes perfect agreement.

YLD124 monomer geometry per chromophore, respectively. Earlier modeling of the optical absorption spectra of YLD124 chromophore aggregates suggests that excitonic states within the aggregates can extend over 10 or more chromophores.⁸⁷ Inclusion of the excitonic interactions in the parametrization of the TSM-MEA and TSM-MEA/ch methods allows to account for the effect of this exciton delocalization on β .

Note that for both dimers and tetramers, the agreement between TSM-MEA and TSM-full is significantly better than the agreement between TSM-sum and TSM-full (average error reduced from 0.131 to 0.033 for dimers and from 0.111 to -0.009 for tetramers; standard deviation also reduced). Although we don't make this comparison for decamers due to computational expense, if the trend persisted, the improvement from including excitonic interactions could be even more significant for larger systems.

The error of first hyperpolarizability calculations using the TSM-MEA or TSM-MEA/ch methods relative to the TSM-full method is smaller than the error of calculations using the TSM-full method relative to the CPHF-full method. Because in all cases errors are not correlated with the first hyperpolarizability values, we expect that using the TSM-MEA or TSM-MEA/ch methods should not produce worse agreement with the CPHF-full method than using the TSM-full method. Indeed, Table 2 shows that the agreement for first hyperpolarizability values calculated using the TSM-full, the TSM-MEA, and the TSM-MEA/ch methods with the values calculated using the CPHF-full method is comparable. This result suggests that if the TSM-full method adequately approximates CPHF-full, the TSM-MEA and TSM-MEA/ch methods should also adequately approximate it.

As discussed in the Methods section, the molecular exciton approximation assumes relatively weak interactions between chromophores. Aggregates of YLD124 chromophores that have large permanent and transition dipole moments pose a particular challenge to the validity of the exciton approximation. Therefore, good performance of the molecular exciton

approximation for calculating the first hyperpolarizability of YLD124 chromophore aggregates would suggest its likely applicability for a wide variety of other chromophore aggregates.

In the following sections, we will further analyze chromophore excitonic interactions and consider how increasing excitonic interactions between chromophores can enhance the first hyperpolarizability of molecular solids.

3.5. First Hyperpolarizability Dependence on Relative Position and Orientation of Chromophores. The agreement between the first hyperpolarizability, β , of chromophore aggregates calculated using different methods depends on the relative position and orientation of chromophores in the aggregate. Figure 9 shows this dependence for pairs of identical YLD124 chromophores (dimers) in select orientations. The chromophore geometry that was used for these calculations can be found in the Supporting Information. Results for additional orientations can be found in Figure S2 in the Supporting Information.

In Figure 9A, the first hyperpolarizability is shown as a function of the distance between the centers of charge of two YLD124 chromophores with the line connecting centers of charge perpendicular to the transition dipole moments for the ground-to-lowest-energy excited-state transition. For this chromophore arrangement, the excitonic coupling between the lowest excited states of the two chromophores produces two dimer excited states, of which the higher one is the bright state (H-aggregate behavior).⁸⁷ In this configuration, the first hyperpolarizability of two noninteracting chromophores would be twice the first hyperpolarizability of a single chromophore. This value is indicated by the black line for the CPHF method and by the brown line for the TSM expression given by eq 8. The offset between the two methods is due to the contribution of states neglected in the TSM expression and can be expected from the error in β of individual chromophores calculated using the TSM expression compared with the CPHF method (Figure 5). At long distances, where interaction between the two chromophores is weak, the first hyperpolarizability of the dimer calculated using all methods approaches the appropriate limit (either CPHF or TSM) of noninteracting chromophores. At smaller interchromophore distances, the first hyperpolarizability of the dimer decreases for all methods, albeit by different amounts. The TSM-MEA results show the smallest decrease in β . The addition of electron density polarization by point charges in the TSM-MEA/ch method leads to a further decrease. The TSM-full results show a sharper decrease in β compared with the CPHF-full results, suggesting that higher lying states will lead to an increase in β rather than the decrease seen with the excitonic interaction of the bright state. For chromophores at a distance of 0.8 nm between their centers of charge (which corresponds to a closest interatomic distance of 2 Å), the decrease in β is 28% for CPHF-full and 29% for TSM-full compared with the noninteracting values. This decrease in β suggests that side-to-side parallel alignment of identical chromophores is not an optimal orientation for maximizing the first hyperpolarizability.

In Figure 9B, the first hyperpolarizability is shown as a function of the distance between the centers of charge of two YLD124 chromophores with the line connecting centers of charge oriented along the transition dipole moments for the ground to lowest-energy excited state. For this chromophore arrangement, the excitonic coupling between the lowest excited states of the two chromophores produces two dimer excited

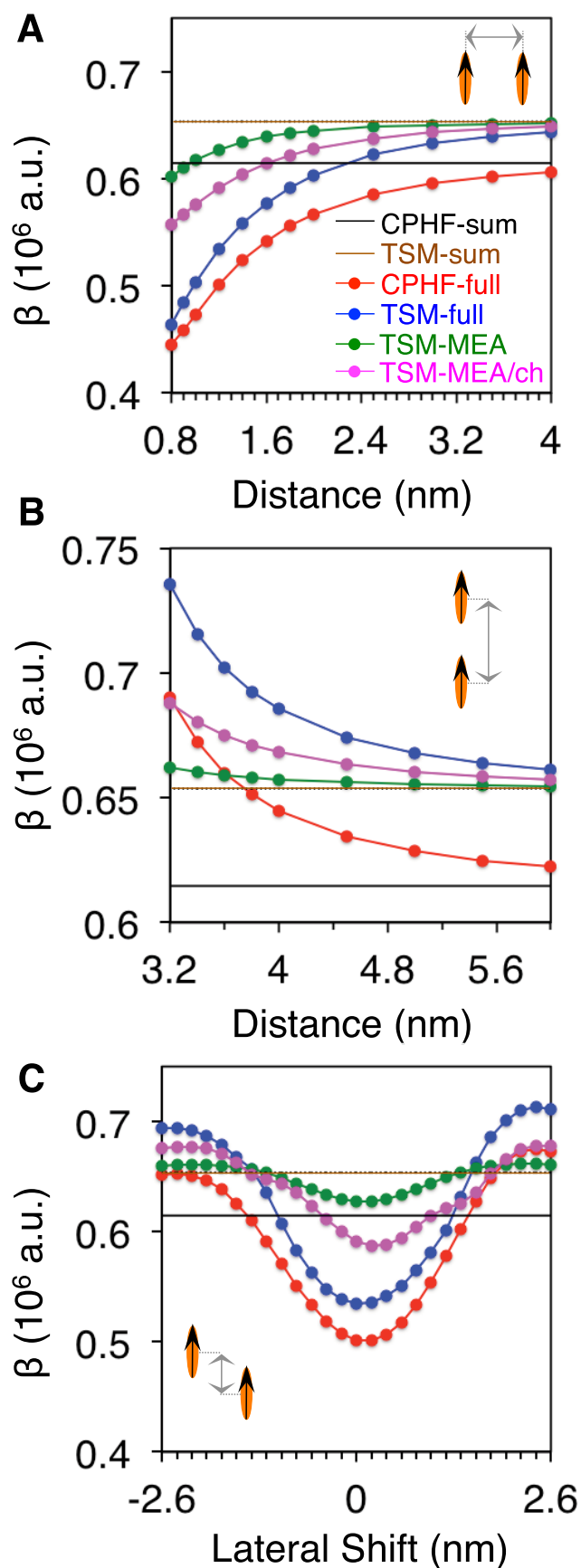


Figure 9. First hyperpolarizabilities calculated for pairs of YLD124 chromophores: red, using the coupled-perturbed Hartree–Fock method (CPHF-full); blue, using the two-state model parametrized based on ab initio calculations on the chromophore pair (TSM-full);

Figure 9. continued

green, using the molecular exciton approximation to the two-state model (TSM-MEA); magenta, using the molecular exciton approximation to the two-state model with the electrostatic environment of the other chromophore represented by its atomic point charges (TSM-MEA/ch). First hyperpolarizability of noninteracting chromophores: black line, calculated using CPHF, brown line, calculated using the TSM. Chromophore arrangements and parameters varied are illustrated in each panel, with black arrows indicating the direction of the chromophore dipole moments.

states, of which the lower one is the bright state (J-aggregate behavior).⁸⁷ At long distances, where interaction between the two chromophores is weak, the first hyperpolarizabilities calculated using all methods approach the values for noninteracting chromophores, like in Figure 9A. However, at smaller interchromophore distances, the first hyperpolarizability of the dimer increases for all methods, rather than decreasing, as in Figure 9A. The TSM-MEA method leads to a small increase in β , with a larger increase upon including point charges in the TSM-MEA/ch method. The TSM-full and CPHF-full methods both predict more substantial increases, with the first hyperpolarizabilities calculated using TSM-full and using CPHF-full tracking very well with each other. For chromophores at a distance of 3.2 nm between their centers of charge (which corresponds to a closest atom–atom distance of 5.126 Å), the increase in β is 12.0% for CPHF-full and 12.6% for TSM-full compared with the values for noninteracting chromophores. This increase in β suggests that head-to-tail parallel alignment of identical chromophores may be an ideal orientation for maximizing the first hyperpolarizability. A similar enhancement of β for head-to-tail chromophore arrangement was predicted by Suponitsky and Masunov⁵⁰ for a crystalline subsystem of chromophores and by Fominykh et al.⁵¹ for azo-chromophore dimers.

Figure 9C shows the first hyperpolarizability of two YLD124 chromophores with transition dipole moments for the ground to lowest-energy excited-state transition oriented along the z -axis as a function of the relative displacement of one of the chromophores with respect to the other along the z -axis from a configuration where the line connecting centers of charge is perpendicular to the z -axis, with a distance of 1.2 nm between centers of charge for noninteracting chromophores at zero displacement. At zero lateral shift, the relative position of chromophores is the same as that at a distance of 1.2 nm in Figure 9A and the value of the first hyperpolarizability for a pair of interacting chromophores is smaller than the sum of the first hyperpolarizabilities of the two chromophores. However, the first hyperpolarizability increases with the absolute magnitude of the lateral shift and eventually exceeds the sum of the first hyperpolarizabilities of the two chromophores, although it does not exceed the value obtained for the head-to-tail orientation at distances between centers of charge less than 4 nm in Figure 9B.

For methods based on the TSM expression for the first hyperpolarizability, eq 8, such behavior can be understood by considering the individual parameters that enter the TSM expression. Figure 10 shows the changes in these parameters as a function of the interchromophore distance for the TSM-full, TSM-MEA, and TSM-MEA/ch calculations, the results of which are shown in Figure 9A. Figure S3 shows the corresponding data for Figure 9B.

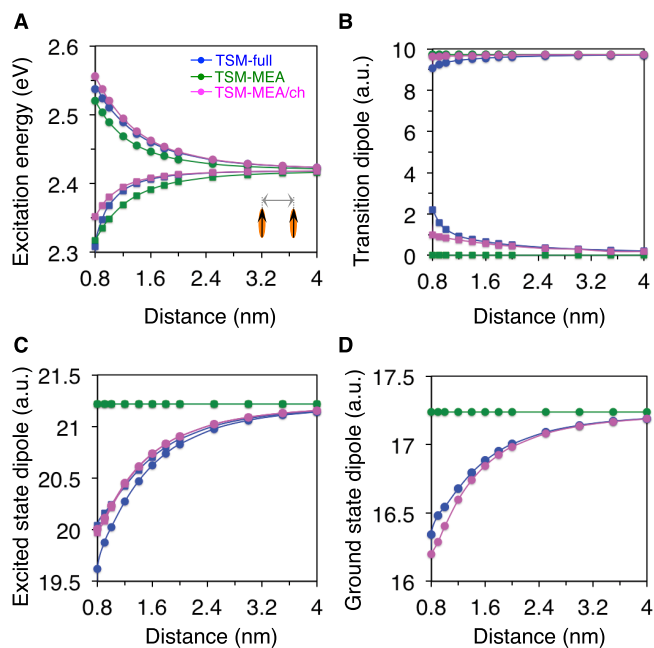


Figure 10. Excitation energy (A) and transition dipole moment (B) for the transitions between the ground and two lowest excited states, as well as the permanent dipole moments of the two excited states (C) and of the ground state (D) for pairs of identical YLD124 chromophores in the configuration corresponding to Figure 9A as a function of the distance between the centers of charge of noninteracting chromophores. Circles: lowest-energy excited state, squares: second-lowest-energy excited state, and diamonds: ground state. Blue: TSM-full, green: TSM-MEA, and magenta: TSM-MEA/ch.

In the TSM-MEA method, the environment of individual chromophores is neglected in the parametrization of the excitonic Hamiltonian. Therefore, the charge distribution on individual chromophores and consequently the ground-state and excited-state dipole moments and transition dipole moments do not depend on the interchromophore distance for this method (green lines in Figure 10B–D). Because both chromophores in the dimer are identical, their noninteracting excitation energies are the same, $\varepsilon_2 = \varepsilon_1$. Taking this fact into account and noting that the transition dipole moments of the two chromophores are parallel in this configuration and the coupling J between them is, therefore, positive, it follows from eqs 5 and 6 in the Supporting Information that in the TSM-MEA method

$$c_1^\pm = \frac{1}{\sqrt{2}}, \quad c_2^\pm = \pm \frac{1}{\sqrt{2}} \quad (22)$$

The higher-energy state (circles in Figure 10) corresponds to the “+” sign in eq 22 and is purely bright in the TSM-MEA method, whereas the lower-energy state (squares in Figure 10) corresponds to the “−” sign and is purely dark (Figure 10B shows that the transition dipole moment between the ground state and this state is zero). The permanent dipole moments of the two excited states of the dimer do not depend on the signs of c_1 and c_2 , are identical in the TSM-MEA method (Figure 10C), and are twice the single-chromophore excited-state dipole moment. The distance dependence of the first hyperpolarizability in the TSM-MEA method is therefore entirely determined by the change in the excitation energy,

Figure 10A, that depends on the interchromophore coupling J according to eq 4 in the Supporting Information.

In the TSM-MEA/ch method (magenta lines in Figure 10), the charge distribution on individual chromophores in the dimer changes with the interchromophore distance due to polarization by the point charges representing the other chromophore. Consequently, in addition to the excitation energies, the ground state, excited state, and transition dipole moments of the dimer also depend on the interchromophore distances. The TSM-MEA/ch results agree well with the TSM-full results (blue lines in Figure 10) at long interchromophore distances, with deviations at shorter distances. These deviations are likely due to an improved description of polarization in the TSM-full method, as well as to interchromophore charge delocalization that is neglected in the TSM-MEA/ch method but can occur in ab initio calculations used to parametrize the TSM-full method. These errors most strongly affect the transition dipole moments (Figure 10B): even at 8 Å distance between the chromophore centers of charge, the errors in the TSM-MEA/ch values of the excitation energies, ground- and excited-state dipole moments, compared with the TSM-full values, do not exceed 2%, whereas the errors in the values for the transition dipole moments are 56% for the lowest-energy (mostly dark) and 6% for the second-lowest-energy (mostly bright) excited states.

From Figure 9, it follows that the first hyperpolarizabilities of chromophore dimers calculated using both the TSM-MEA/ch and the TSM-MEA methods agree reasonably well with those calculated using the TSM-full method for interchromophore distances $\gtrsim 1$ nm. Such interchromophore distances are typical for disordered chromophore aggregates like the ones considered in this paper, and the first hyperpolarizability of such systems may be calculated using the molecular exciton model. Note that the excitonic enhancement or suppression of the first hyperpolarizability due to the interaction of chromophores in a dimer is larger when both chromophores are identical, because equal excitation energies for both chromophores allow for the greatest delocalization of excited states within the dimer.

In the following section, we will extend the considerations regarding the arrangement of chromophores that maximizes electro-optic response to infinite periodic systems.

3.6. First Hyperpolarizability for Periodic Arrays of Chromophores. The TSM within the molecular exciton approximation can be used to calculate the first hyperpolarizability for periodic arrays of aligned chromophores (molecular crystals) analytically. In this section, we present this calculation for a one-dimensional molecular crystal (the extension to crystals of higher dimensionality is analogous to standard band theory).¹⁰³

Note that in molecular crystals, YLD124 molecules form π -stacked, centrosymmetrically ordered sheets with a stacking distance of about 4 Å. Because the structure is centrosymmetric, there is no electro-optic activity. Within a plane, donors are adjacent to acceptors. The side-to-side N–H distance for chromophores in adjacent planes is about 2.4 to 3.2 Å, and the H–F distance is about 3 Å. The closest C–C distance between carbon atoms in the donor moieties for chromophores within a sheet is about 3.9 Å;¹⁰⁴ because chromophores are arranged centrosymmetrically, donors are adjacent to donors and acceptors are adjacent to acceptors. At such small interchromophore distances, charge transfer between YLD124 chromophores may be non-negligible. Therefore, before calculating the

first hyperpolarizability of a molecular crystal using the approach described in this section, the validity of the exciton model for that crystal must be verified.

Consider a one-dimensional array that consists of N identical chromophores with distance a between nearest-neighbor chromophores and periodic boundary conditions. The periodic boundary conditions require that the wavevector of this system obey the condition

$$|\Psi(x)\rangle = |\Psi(x + Na)\rangle \quad (23)$$

Because all chromophores are identical, all observables at points separated by an integer number of lattice constants a must be identical. Therefore, e.g., the excitation density must satisfy the condition

$$\begin{aligned} \rho(x + a) &= |\Psi(x + a)\rangle\langle\Psi(x + a)| = |\Psi(x)\rangle\langle\Psi(x)| \\ &= \rho(x) \end{aligned} \quad (24)$$

This condition is only satisfied if

$$|\Psi(x + a)\rangle = \exp(i\varphi)|\Psi(x)\rangle \quad (25)$$

where φ is a phase shift in the wavevector between any pair of neighboring chromophores. When the phase shift in eq 25 is applied N times, the periodic boundary condition given by eq 23 requires that

$$|\Psi(x + Na)\rangle = \exp(i\varphi N)|\Psi(x)\rangle = |\Psi(x)\rangle \quad (26)$$

This condition can only be satisfied if

$$\varphi = ka \quad (27)$$

where we defined the wavenumber k as

$$k = \frac{2\pi n}{Na} \quad (28)$$

with $n \in \mathbb{Z}$.

In the molecular exciton approximation, any wavevector $|\Psi\rangle$ in the manifold of eigenstates that are constructed from the lowest excited states of individual chromophores can be expanded according to eq 11, where the basis $\{|\Phi_j\rangle: j = 1, \dots, N\}$, is given by eq 12. By construction, there is no spatial overlap between the basis functions $|\Phi_l\rangle$ and $|\Phi_m\rangle$ for all $l \neq m$: $\langle\Phi_l|\Phi_m\rangle = \delta_{lm}$. Therefore, at any point x , the Hamiltonian eigenvector $|\Psi\rangle$ is only determined by one basis function.

Due to translational symmetry, basis functions for identical chromophores at different sites in the array can be obtained from one another simply by shifting their position: $|\Phi_{l+ma}(x)\rangle = |\Phi_l(x + ma)\rangle$. Therefore, the phase difference in the wavevector $|\Psi\rangle$ between sites is entirely determined by the coefficients in the wavefunction expansion in eq 11. Because all sites in the array are equivalent, the magnitudes of all coefficients in this expansion are the same. We will select the coefficient at site 1 to be real, $c_1 = N^{-1/2}$, where N is the number of chromophores in the array. According to eq 25, the coefficient at site n then has to be

$$c_n = N^{-1/2} \exp[ik(n - 1)a] \quad (29)$$

The prefactor $N^{-1/2}$ in eq 29 ensures that the coefficients c_n satisfy the normalization condition

$$\sum_{n=1}^N |c_n|^2 = 1$$

If only interactions between nearest-neighbor chromophores in the array are included in the Hamiltonian, then from eq 9 it follows that

$$\omega c_n + Jc_{n-1} + Jc_{n+1} = Ec_n \quad (30)$$

where ω is the excitation energy of an individual chromophore and J is the excitonic coupling between nearest-neighbor chromophores. Introducing eq 29 into eq 30 gives

$$\begin{aligned} N^{-1/2}\omega \exp[ik(n - 1)a] + N^{-1/2}J \exp[ik(n - 2)a] \\ + N^{-1/2}J \exp[ikna] \\ = N^{-1/2}E \exp[ik(n - 1)a] \end{aligned}$$

and therefore the dispersion relation for the one-excitation band is

$$E(k) = \omega + 2J \frac{\exp(ika) + \exp(-ika)}{2} = \omega + 2J \cos(ka) \quad (31)$$

The oscillator strength that corresponds to the transition from the ground state of the chromophore array to the excited state that corresponds to the wavevector k is given by⁸⁷

$$f(k) = \frac{2m}{3e^2\hbar^2} E(k) \sum_{\alpha=x,y,z} \left| \sum_{n=1}^N c_n(k) \mu_n^{\alpha(\text{ge})} \right| \quad (32)$$

where m is the electron mass, e is the elementary charge, \hbar is the reduced Planck constant, $c_n(k)$ is the expansion coefficient that describes the contribution of the n th chromophore in the array to the eigenstate with wavenumber k , and μ_n^{α} (ge) is the α component of the transition dipole moment between the ground and the excited state of the n th chromophore in the array.

Introducing eqs 31 and 29 into eq 32 and evaluating the sum of the geometric series

$$\sum_{n=1}^N \exp[ik(n - 1)a] = \frac{1 - \exp(ikNa)}{1 - \exp(ika)} = \exp\left[\frac{ika(N - 1)}{2}\right] \frac{\sin\left(\frac{kNa}{2}\right)}{\sin\left(\frac{ka}{2}\right)}$$

results in the following expression for the oscillator strength

$$f(k) = \frac{2m}{3e^2\hbar^2} [\omega + 2J \cos(ka)] \frac{\sin^2\left(\frac{kNa}{2}\right)}{\sin^2\left(\frac{ka}{2}\right)} \sum_{\alpha=x,y,z} \mu_n^{\alpha(\text{ge})} \quad (33)$$

Introducing the value of the wavenumber given by eq 28 into eq 33 gives an oscillator strength of 0 for all values of k except $k = 0$, for which the expression given by eq 33 is indeterminate. Resolving this indeterminacy by l'Hôpital's rule gives a finite value of the oscillator strength for $k = 0$

$$f(0) = \frac{2mN}{3e^2\hbar^2} (\omega + 2J) \sum_{\alpha=x,y,z} \mu_n^{\alpha(\text{ge})} \quad (34)$$

The array of chromophores has only a single bright state for $k = 0$; therefore, its first hyperpolarizability can be calculated using the two-state model expression, eq 8, for that bright state. The ground state, excited state, and transition dipole moments that enter eq 8 can be evaluated within the molecular exciton approximation using eqs 13–15 and 18, with the expansion coefficients for the bright excited eigenstate given by eq 29

$$\begin{aligned}\vec{\mu}^{|\Psi_0\rangle} &= \vec{\mu}^g N, \vec{\mu}^{|\Psi_0\rangle} = [\vec{\mu}^e + (N-1)\vec{\mu}^g], \vec{\mu}^{|\Psi_0\rangle \rightarrow |\Psi_0\rangle} \\ &= \vec{\mu}^{ge} N^{1/2}\end{aligned}\quad (35)$$

Introducing eqs 31 and 35 into eq 8, we arrive at the final expression for the first hyperpolarizability tensor

$$\beta_{\eta\kappa\lambda} = \frac{2N\mu_{\eta}^{ge}\mu_{\kappa}^{ge}[\mu_{\lambda}^e - \mu_{\lambda}^g]}{(\epsilon + 2J)^2}\quad (36)$$

The factor N in this expression indicates that the first hyperpolarizability scales linearly with the number of identical chromophores in the array. If the excitonic coupling, J , is negligible, the first hyperpolarizability of the chromophore array is simply the sum of the first hyperpolarizabilities of individual chromophores. If the excitonic coupling is positive, then the first hyperpolarizability of the array is suppressed compared with the case of noninteracting chromophores, and if the excitonic coupling is negative, the first hyperpolarizability of the array is enhanced compared with the case of noninteracting chromophores.

For chromophores with parallel transition dipole moments, excitonic couplings are positive in a side-by-side configuration and negative in a head-to-tail configuration. Therefore, the results obtained here for periodic arrays of chromophores are consistent with the trends seen for pairs of chromophores in side-by-side and head-to-tail configurations that we discussed in the previous section. Generally, to obtain a superlinear enhancement of the first hyperpolarizability with the number of chromophores, the chromophores should be positioned in a head-to-tail configuration. This chromophore arrangement corresponds to a J-aggregate signature in linear spectroscopy. Therefore, J-aggregation is beneficial to enhancing the first hyperpolarizability of chromophore aggregates and molecular crystals and linear spectroscopy may provide insights into the first hyperpolarizability of chromophore assemblies. Periodic molecular crystals allow for maximal superlinearity of the first hyperpolarizability dependence on the number of chromophores, because the absence of energetic disorder within the crystal allows for maximum delocalization of excitations within the crystal.

4. CONCLUSIONS

In this paper, we apply the TSM within the molecular exciton approximation to compute the first hyperpolarizability, β , of both disordered and ordered chromophore aggregates. Our method accounts for excitonic interactions between chromophores while only requiring electronic structure calculations on single chromophores. Consequently, it enables computationally affordable calculations of the electro-optic response of bulk disordered or crystalline organic materials.

The TSM as implemented here only accounts for the effect of the ground- to lowest-energy bright excited-state transition of individual chromophores. To assess the effects of transitions involving higher-energy states on β , we compared calculations using the TSM to those using the more rigorous CPHF method. Our calculations on disordered chromophore aggregates show that the geometries of individual chromophores substantially influence the β value of the aggregate and should be accounted for if possible. For aggregates of two or four chromophores, the errors that result from making the TSM approximation exceed the errors that result from ignoring excitonic interactions between individual chromophores when taking a tensor sum of their first hyperpolarizabilities calculated

using the CPHF method. However, adding excitonic effects to the TSM within the molecular exciton approximation improves agreement with the more rigorous CPHF results and does not appear to introduce substantial errors beyond those inherent to the TSM. Because of computational expense, we did not compute the first hyperpolarizabilities using the CPHF method for aggregates consisting of more than four chromophores. However, we compared the values of β calculated using the TSM within the molecular exciton approximation and using the TSM with excitonic interactions between chromophores neglected. Excitonic interactions altered the first hyperpolarizability to a greater degree for larger chromophore aggregates, suggesting that excitonic effects become more pronounced in larger systems. The dependence of excitonic effects on the first hyperpolarizability of the aggregate seems to depend nearly linearly on the size of the system, at least for aggregate sizes between 2 and 10 chromophores. The average reduction in the first hyperpolarizability magnitude per chromophore in this range is on average 12–14% of the magnitude of the first hyperpolarizability for the optimized geometry of a YLD124 chromophore.

For pairs of YLD124 chromophores in their optimized geometry, we examined the trends in the computed β values as a function of distance and relative orientation. We found that the TSM captured the trends observed when using the CPHF method: e.g., side-by-side chromophore alignment leading to a decrease in β and head-to-tail alignment leading to an enhancement in β . The molecular exciton approximation to the TSM was able to track the same trends when parametrized with values of excitation energies and transition densities computed in the presence of atomic charges to account for interchromophore polarization. Our analysis of the first hyperpolarizability of chromophore dimers for a variety of relative orientations suggests that β can be enhanced beyond a simple tensor sum by means of head-to-tail alignment of chromophores and that this enhancement is due to both interchromophore polarization and excitonic coupling between chromophores. This result agrees with previous analysis by Suponitsky and Masunov.⁵⁰

We also present a way to analytically calculate the first hyperpolarizability of a one-dimensional periodic array of chromophores within the molecular exciton approximation to the TSM. The obtained expression for β predicts the orientations of chromophores that enhance and decrease the electro-optic response. Although we have not yet validated this expression by comparison with all-electron calculations, this technique presents a promising way for including an approximate correction for excitonic effects in periodic systems.

This study presents a way forward for simulating the electro-optic response of disordered and ordered organic materials that takes into account interactions between chromophores. We quantify the extent of the changes in β due to excitonic interactions and to polarization of the electron density of chromophores by their electrostatic environment in small aggregates. We suggest that head-to-tail alignment of chromophores would provide an ideal design strategy for excitonic enhancement of β in organic electro-optic materials.

■ ASSOCIATED CONTENT

Supporting Information

The Supporting Information is available free of charge on the ACS Publications website at DOI: 10.1021/acs.jpcc.8b12445.

TSM for computing the first hyperpolarizability of chromophore aggregates; additional results for interacting chromophore dimers; sample CPHF and TDDFT/TSM data for the optimized geometry of the YLD124 chromophore (PDF)

AUTHOR INFORMATION

Corresponding Authors

*E-mail: aleksey.kocherzhenko@csueastbay.edu (A.A.K.).

*E-mail: cisborn@ucmerced.edu (C.M.I.).

ORCID

Lewis E. Johnson: 0000-0002-7412-073X

Christine M. Isborn: 0000-0002-4905-9113

Author Contributions

[†]This manuscript has been authored by UT-Battelle, LLC under Contract No. DE-AC05-00OR22725 with the U.S. Department of Energy. The United States Government retains and the publisher, by accepting the article for publication, acknowledges that the United States Government retains a nonexclusive, paid-up, irrevocable, worldwide license to publish or reproduce the published form of this manuscript, or allow others to do so, for United States Government purposes. The Department of Energy will provide public access to these results of federally sponsored research in accordance with the DOE Public Access Plan (<http://energy.gov/downloads/doe-public-access-plan>).

Funding

L.E.J. was supported by the Air Force Office of Scientific Research (FA9550-15-1-0319) and National Science Foundation (DMR-1303080); Any opinions, findings, and conclusions or recommendations expressed in this article are those of the author(s) and do not necessarily reflect the views of the National Science Foundation.

Notes

The authors declare no competing financial interest.

ACKNOWLEDGMENTS

This work was supported by the U.S. Department of Defense (Proposal 67310-CH-REP) under the Air Force Office of Scientific Research Organic Materials Division. AFT has been partially supported by the U.S. Department of Energy, Office of Science, Office of Advanced Scientific Computing Research, Oak Ridge Leadership Computing facility under contract number DE-AC05-00OR22725. This work used the MERCED computational resource supported by the NSF MRI Program (Grant ACI-1429783). We thank Professor Bruce Robinson for helpful discussions.

REFERENCES

- (1) Kanis, D. R.; Ratner, M. A.; Marks, T. J. Design and Construction of Molecular Assemblies with Large Second-Order Optical Nonlinearities. Quantum Chemical Aspects. *Chem. Rev.* **1994**, *94*, 195–242.
- (2) Dalton, L. R.; Steier, W. H.; Robinson, B. H.; Zhang, C.; Ren, A.; Garner, S.; Chen, A.; Londergan, T.; Irwin, L.; Carlson, B.; et al. From Molecules to Opto-Chips: Organic Electro-Optic Materials. *J. Mater. Chem.* **1999**, *9*, 1905–1920.
- (3) Marder, S. R. Organic Nonlinear Optical Materials: Where We Have Been and Where We Are Going. *Chem. Commun.* **2006**, 131–134.
- (4) Reed, G. T.; Mashanovich, G.; Gardes, F. Y.; Thomson, D. J. Silicon Optical Modulators. *Nat. Photonics* **2010**, *4*, 518–526.

- (5) Dalton, L. R.; Sullivan, P. A.; Bale, D. H. Electric Field Poled Organic Electro-optic Materials: State of the Art and Future Prospects. *Chem. Rev.* **2010**, *110*, 25–55.

- (6) Chen, A.; Murphy, E. J. *Broadband Optical Modulators: Science, Technology, and Applications*; CRC Press/Taylor & Francis Group: Boca Raton, 2012.

- (7) Kuzyk, M. G.; Perez-Moreno, J.; Shafei, S. Sum Rules and Scaling in Nonlinear Optics. *Phys. Rep.* **2013**, *529*, 297–398.

- (8) Dalton, L. R. et al. *Organic Electro-Optics and Photonics: Molecules, Polymers and Crystals*; Cambridge University Press, 2015.

- (9) Liu, J.; Xu, G.; Liu, F.; Kityk, I.; Liu, X.; Zhen, Z. Recent Advances in Polymer Electro-Optic Modulators. *RSC Adv.* **2015**, *5*, 15784–15794.

- (10) Koos, C.; Leuthold, J.; Freude, W.; Kohl, M.; Dalton, L.; Bogaerts, W.; Giesecke, A. L.; Lauer, M.; Melikyan, A.; Koeber, S.; et al. Silicon-Organic Hybrid (SOH) and Plasmonic-Organic Hybrid (POH). *J. Lightwave Technol.* **2016**, *34*, 256–268.

- (11) Heni, W.; Haffner, C.; Elder, D. L.; Tillack, A. F.; Fedoryshyn, Y.; Cottier, R.; Salamin, Y.; Hoessbacher, C.; Koch, U.; Cheng, B.; et al. Nonlinearities of Organic Electro-Optic Materials in Nanoscale Slots and Implications for the Optimum Modulator Design. *Opt. Express* **2017**, *25*, 2627–2653.

- (12) Zyss, J.; Oudar, J. L. Relations Between Microscopic and Macroscopic Lowest-Order Optical Nonlinearities of Molecular Crystals With One- or Two-Dimensional Units. *Phys. Rev. A* **1982**, *26*, 2028–2048.

- (13) González-Urbina, L.; Baert, K.; Kolaric, B.; Perez-Moreno, J.; Clays, K. Linear and Nonlinear Optical Properties of Colloidal Photonic Crystals. *Chem. Rev.* **2012**, *112*, 2268–2285.

- (14) Schneider, A.; Neis, M.; Stillhart, M.; Ruiz, B.; Khan, R. U. A.; Günter, P. Generation of Terahertz Pulses Through Optical Rectification in Organic DAST Crystals: Theory and Experiment. *J. Opt. Soc. Am. B* **2006**, *23*, 1822–1835.

- (15) Jazbinsek, M.; Mutter, L.; Gunter, P. Photonic Applications With the Organic Nonlinear Optical Crystal DAST. *IEEE J. Sel. Top. Quantum Electron.* **2008**, *14*, 1298–1311.

- (16) Yi, Y.; Coropceanu, V.; Bredas, J.-L. Exciton-Dissociation and Charge-Recombination Processes in Pentacene/C60 Solar Cells: Theoretical Insight into the Impact of Interface Geometry. *J. Am. Chem. Soc.* **2009**, *131*, 15777–15783.

- (17) Heimel, G.; Salzmann, I.; Duhm, S.; Rabe, J. P.; Koch, N. Intrinsic Surface Dipoles Control the Energy Levels of Conjugated Polymers. *Adv. Funct. Mater.* **2009**, *19*, 3874–3879.

- (18) Marchiori, C.; Koehler, M. Dipole Assisted Exciton Dissociation at Conjugated Polymer/Fullerene Photovoltaic Interfaces: A Molecular Study Using Density Functional Theory calculations. *Synth. Methods* **2010**, *160*, 643–650.

- (19) Ojala, A.; Petersen, A.; Fuchs, A.; Lovrincic, R.; Polking, C.; Trollmann, J.; Hwang, J.; Lennartz, C.; Reichelt, H.; Hoffken, H. W.; et al. Merocyanine/C60 Planar Heterojunction Solar Cells: Effect of Dye Orientation on Exciton Dissociation and Solar Cell Performance. *Adv. Funct. Mater.* **2012**, *22*, 86–96.

- (20) Yost, S. R.; van Voorhis, T. Electrostatic Effects at Organic Semiconductor Interfaces: A Mechanism for Cold Exciton Breakup. *J. Phys. Chem. C* **2013**, *117*, 5617–5625.

- (21) Ran, N. A.; Roland, S.; Love, J. A.; Savikhin, V.; Takacs, C. J.; Fu, Y.-T.; Li, H.; Coropceanu, V.; Liu, X.; Brédas, J.-L.; et al. Impact of Interfacial Molecular Orientation on Radiative Recombination and Charge Generation Efficiency. *Nat. Commun.* **2017**, *8*, No. 79.

- (22) Kohn, A. W.; McMahon, D. P.; Wen, S.; van Voorhis, T. The Impact of Carrier Delocalization and Interfacial Electric Field Fluctuations on Organic Photovoltaics. *J. Phys. Chem. C* **2017**, *121*, 26629–26636.

- (23) Lee, H.; Lee, D.; Sin, D. H.; Kim, S. W.; Jeong, M. S.; Cho, K. Effect of Donor-Acceptor Molecular Orientation on Charge Photo-generation in Organic Solar Cells. *NPG Asia Mater* **2018**, *10*, 469–481.

- (24) Di Bella, S.; Ratner, M. A.; Marks, T. J. Design of Chromophoric Molecular Assemblies With Large Second-Order

Optical Nonlinearities. A Theoretical Analysis of the Role of Intermolecular Interactions. *J. Am. Chem. Soc.* **1992**, *114*, 5842–5849.

(25) Yokoyama, S.; Nakahama, T.; Otomo, A.; Mashiko, S. Intermolecular Coupling Enhancement of the Molecular Hyperpolarizability in Multichromophoric Dipolar Dendrons. *J. Am. Chem. Soc.* **2000**, *122*, 3174–3181.

(26) Bartholomew, G. P.; Ledoux, I.; Mukamel, S.; Bazan, G. C.; Zyss, J. Three-Dimensional Nonlinear Optical Chromophores Based on Through-Space Delocalization. *J. Am. Chem. Soc.* **2002**, *124*, 13480–13485.

(27) Liao, Y.; Firestone, K. A.; Bhattacharjee, S.; Luo, J.; Haller, M.; Hau, S.; Anderson, C. A.; Lao, D.; Eichinger, B. E.; Robinson, B. H.; et al. Linear and Nonlinear Optical Properties of a Macrocyclic Trichromophore Bundle with Parallel-Aligned Dipole Moments. *J. Phys. Chem. B* **2006**, *110*, 5434–5438.

(28) Benight, S. J.; Johnson, L. E.; Barnes, R.; Olbricht, B. C.; Bale, D. H.; Reid, P. J.; Eichinger, B. E.; Dalton, L. R.; Sullivan, P. A.; Robinson, B. H. Reduced Dimensionality in Organic Electro-Optic Materials: Theory and Defined Order. *J. Phys. Chem. B* **2010**, *114*, 11949–11956.

(29) Dalton, L. R.; Benight, S. J.; Johnson, L. E.; Knorr, D. B.; Kosilkin, I.; Eichinger, B. E.; Robinson, B. H.; Jen, A. K.-Y.; Overney, R. M. Systematic Nanoengineering of Soft Matter Organic Electro-optic Materials. *Chem. Mater.* **2011**, *23*, 430–445.

(30) Isborn, C. M.; Leclercq, A.; Vila, F. D.; Dalton, L. R.; Bredas, J. L.; Eichinger, B. E.; Robinson, B. H. Comparison of Static First Hyperpolarizabilities Calculated with Various Quantum Mechanical Methods. *J. Phys. Chem. A* **2007**, *111*, 1319–1327.

(31) Suponitsky, K. Y.; Tafur, S.; Masunov, A. E. Applicability of Hybrid Density Functional Theory Methods to Calculation of Molecular Hyperpolarizability. *J. Chem. Phys.* **2008**, *129*, No. 044109.

(32) Champagne, B. *Chemical Modelling: Applications and Theory*; The Royal Society of Chemistry, 2009; Vol. 6, pp 17–62.

(33) de Wergifosse, M.; Champagne, B. Electron Correlation Effects on the First Hyperpolarizability of Push–Pull π -Conjugated Systems. *J. Chem. Phys.* **2011**, *134*, No. 074113.

(34) Champagne, B.; Beaujean, P.; de Wergifosse, M.; Cardenuto, M. H.; Liégeois, V.; Castet, F. In *Frontiers of Quantum Chemistry*; Wójcik, M. J., Nakatsuji, H., Kirtman, B., Ozaki, Y., Eds.; Springer: Singapore, 2018; pp 117–138.

(35) Garrett, K.; Sosa Vazquez, X.; Egri, S. B.; Wilmer, J.; Johnson, L. E.; Robinson, B. H.; Isborn, C. M. Optimum Exchange for Calculation of Excitation Energies and Hyperpolarizabilities of Organic Electro-optic Chromophores. *J. Chem. Theory Comput.* **2014**, *10*, 3821–3831.

(36) Johnson, L. E.; Dalton, L. R.; Robinson, B. H. Optimizing Calculations of Electronic Excitations and Relative Hyperpolarizabilities of Electrooptic Chromophores. *Acc. Chem. Res.* **2014**, *47*, 3258–3265.

(37) Garza, A. J.; Wazzan, N. A.; Asiri, A. M.; Scuseria, G. E. Can Short- and Middle-Range Hybrids Describe the Hyperpolarizabilities of Long-Range Charge-Transfer Compounds? *J. Phys. Chem. A* **2014**, *118*, 11787–11796.

(38) Parker, S. M.; Rappoport, D.; Furche, F. Quadratic Response Properties from TDDFT: Trials and Tribulations. *J. Chem. Theory Comput.* **2018**, *14*, 807–819.

(39) Shi, Y.; Zhang, C.; Zhang, H.; Bechtel, J. H.; Dalton, L. R.; Robinson, B. H.; Steier, W. H. Low (Sub-1-Volt) Halfwave Voltage Polymeric Electro-optic Modulators Achieved by Controlling Chromophore Shape. *Science* **2000**, *288*, 119–122.

(40) Jen, A.; Luo, J.; Kim, T.-D.; Chen, B.; Jang, S.-H.; Kang, J.-W.; Tucker, N. M.; Hau, S.; Tian, Y.; Ka, J.-W. et al. In *Exceptional Electro-Optic Properties Through Molecular Design and Controlled Self-Assembly*, Proceeding of SPIE 5935, Linear and Non-linear Optics of Organic Materials V; International Society for Optics and Photonics, 2005; p 593506.

(41) Gajdoš, M.; Hummer, K.; Kresse, G.; Furthmüller, J.; Bechstedt, F. Linear Optical Properties in the Projector-Augmented Wave Methodology. *Phys. Rev. B* **2006**, *73*, No. 045112.

(42) Ferrero, M.; Rerat, M.; Orlando, R.; Dovesi, R. The Calculation of Static Polarizabilities of 1-3D Periodic Compounds. The Implementation in the Crystal Code. *J. Comput. Chem.* **2008**, *29*, 1450–1459.

(43) Ferrero, M.; Rerat, M.; Kirtman, B.; Dovesi, R. Calculation of First and Second Static Hyperpolarizabilities of One- to Three-Dimensional Periodic Compounds. Implementation in the CRYSTAL Code. *J. Chem. Phys.* **2008**, *129*, No. 244110.

(44) Orlando, R.; Lacivita, V.; Bast, R.; Ruud, K. Calculation of the First Static Hyperpolarizability Tensor of Three-Dimensional Periodic Compounds with a Local Basis Set: A Comparison of LDA, PBE, PBEO, B3LYP, and HF Results. *J. Chem. Phys.* **2010**, *132*, No. 244106.

(45) Maschio, L.; Rerat, M.; Kirtman, B.; Dovesi, R. Calculation of the Dynamic First Electronic Hyperpolarizability of Periodic Systems. Theory, Validation, and Application to Multi-Layer MoS₂. *J. Chem. Phys.* **2015**, *143*, No. 244102.

(46) Perdew, J. P.; Burke, K.; Ernzerhof, M. Generalized Gradient Approximation Made Simple. *Phys. Rev. Lett.* **1996**, *77*, 3865–3868.

(47) Heyd, J.; Scuseria, G.; Ernzerhof, M. Hybrid Functionals Based on a Screened Coulomb Potential. *J. Chem. Phys.* **2003**, *118*, 8207–8215.

(48) Onida, G.; Reining, L.; Rubio, A. Electronic Excitations: Density-Functional versus Many-Body Green's-Function Approaches. *Rev. Mod. Phys.* **2002**, *74*, 601–659.

(49) Munn, R. W. Exciton effects in the nonlinear optical susceptibilities of molecular crystals. *J. Chem. Phys.* **1997**, *106*, 3870–3875.

(50) Suponitsky, K. Y.; Masunov, A. E. Supramolecular Step in Design of Nonlinear Optical Materials: Effect of $\pi\cdots\pi$ Stacking Aggregation on Hyperpolarizability. *J. Chem. Phys.* **2013**, *139*, No. 094310.

(51) Fominykh, O. D.; Sharipova, A. V.; Yu. Balakina, M. The Choice of Appropriate Density Functional for the Calculation of Static First Hyperpolarizability of Azochromophores and Stacking Dimers. *Int. J. Quantum Chem.* **2016**, *116*, 103–112.

(52) Castet, F.; Champagne, B. Simple Scheme To Evaluate Crystal Nonlinear Susceptibilities: Semiempirical AM1 Model Investigation of 3-Methyl-4-Nitroaniline Crystal. *J. Phys. Chem. A* **2001**, *105*, 1366–1370.

(53) Seidler, T.; Stadnicka, K.; Champagne, B. Second-order Nonlinear Optical Susceptibilities and Refractive Indices of Organic Crystals from a Multiscale Numerical Simulation Approach. *Adv. Opt. Mater.* **2014**, *2*, 1000–1006.

(54) Seidler, T.; Krawczuk, A.; Champagne, B.; Stadnicka, K. QTAIM-Based Scheme for Describing the Linear and Nonlinear Optical Susceptibilities of Molecular Crystals Composed of Molecules with Complex Shapes. *J. Phys. Chem. C* **2016**, *120*, 4481–4494.

(55) Chemla, D. S.; Oudar, J. L.; Jerphagnon, J. Origin of the Second-Order Optical Susceptibilities of Crystalline Substituted Benzene. *Phys. Rev. B* **1975**, *12*, 4534–4546.

(56) Johnson, L. E.; Elder, D. L.; Kocherzhenko, A. A.; Isborn, C. M.; Dalton, L. R.; Robinson, B. H. In *Poling-Induced Birefringence in OEO Materials Under Nanoscale Confinement*, Proceeding of SPIE, Organic and Hybrid Sensors and Bioelectronics XI; International Society for Optics and Photonics, 2018; p 107381A.

(57) Gerratt, J.; Mills, I. M. Force Constants and Dipole-Moment Derivatives of Molecules from Perturbed Hartree–Fock Calculations. I. *J. Chem. Phys.* **1968**, *49*, 1719–1729.

(58) Pulay, P. Ab Initio Calculation of Force Constants and Equilibrium Geometries in Polyatomic Molecules. *Mol. Phys.* **1969**, *17*, 197–204.

(59) Pople, J. A.; Krishnan, R.; Schlegel, H. B.; Binkley, J. S. Derivative Studies in Hartree–Fock and Möller–Plesset Theories. *Int. J. Quantum Chem.* **1979**, *16*, 225–241.

(60) Dykstra, C. E.; Jasien, P. G. Derivative Hartree–Fock theory to all orders. *Chem. Phys. Lett.* **1984**, *109*, 388–393.

(61) Sekino, H.; Bartlett, R. J. Frequency Dependent Nonlinear Optical Properties of Molecules. *J. Chem. Phys.* **1986**, *85*, 976–989.

- (62) Orr, B.; Ward, J. Perturbation Theory of the Non-Linear Optical Polarization of an Isolated System. *Mol. Phys.* **1971**, *20*, 513–526.
- (63) Oudar, J. L.; Chemla, D. S. Hyperpolarizabilities of the Nitroanilines and Their Relations to the Excited State Dipole Moment. *J. Chem. Phys.* **1977**, *66*, 2664–2668.
- (64) Oudar, J. L. Optical Nonlinearities of Conjugated Molecules. Stilbene Derivatives and Highly Polar Aromatic Compounds. *J. Chem. Phys.* **1977**, *67*, 446–457.
- (65) Nandi, P.; Chattopadhyay, T.; Bhattacharyya, S. Theoretical Study of Solvent Modulation of the First Hyperpolarizability of PNA, DNBT and DCH. *J. Mol. Struct.: THEOCHEM* **2001**, *545*, 119–129.
- (66) Berkovic, G.; Meshulam, G.; Kotler, Z. Measurement and Analysis of Molecular Hyperpolarizability in the Two-Photon Resonance Regime. *J. Chem. Phys.* **2000**, *112*, 3997–4003.
- (67) Benassi, E.; Egidi, F.; Barone, V. General Strategy for Computing Nonlinear Optical Properties of Large Neutral and Cationic Organic Chromophores in Solution. *J. Phys. Chem. B* **2015**, *119*, 3155–3173.
- (68) Katariya, S. B.; Patil, D.; Rhyman, L.; Alswaidan, I. A.; Ramasami, P.; Sekar, N. Triphenylamine-Based Fluorescent NLO Phores With ICT Characteristics: Solvatochromic and Theoretical Study. *J. Mol. Struct.* **2017**, *1150*, 493–506.
- (69) Tathe, A. B.; Sekar, N. Red Emitting NLOphoric 3-Styryl Coumarins: Experimental and Computational Studies. *Opt. Mater.* **2016**, *51*, 121–127.
- (70) Buckley, L. E. R.; Coe, B. J.; Rusanova, D.; Joshi, V. D.; Sanchez, S.; Jirasek, M.; Vavra, J.; Khobragade, D.; Severa, L.; Cisarova, I.; et al. Tunable Chiral Second-Order Nonlinear Optical Chromophores Based on Helquat Dications. *J. Phys. Chem. A* **2017**, *121*, 5842–5855.
- (71) Cesaretti, A.; Carlotti, B.; Elisei, F.; Fortuna, C. G.; Spalletti, A. Photoinduced ICT vs. Excited Rotamer Intercoversion in Two Quadrupolar Polyaromatic N-Methylpyridinium Cations. *Phys. Chem. Chem. Phys.* **2018**, *20*, 2851–2864.
- (72) Hendrickx, E.; Clays, K.; Persoons, A.; Dehu, C.; Bredas, J. L. The Bacteriorhodopsin Chromophore Retinal and Derivatives: An Experimental and Theoretical Investigation of the Second-Order Optical Properties. *J. Am. Chem. Soc.* **1995**, *117*, 3547–3555.
- (73) Meyers, F.; Marder, S. R.; Pierce, B. M.; Bredas, J. L. Electric Field Modulated Nonlinear Optical Properties of Donor-Acceptor Polyenes: Sum-Over-States Investigation of the Relationship between Molecular Polarizabilities (α , β , and γ) and Bond Length Alternation. *J. Am. Chem. Soc.* **1994**, *116*, 10703–10714.
- (74) Momicchioli, F.; Ponterini, G.; Vanossi, D. First- and Second-Order Polarizabilities of Simple Merocyanines. An Experimental and Theoretical Reassessment of the Two-Level Model. *J. Phys. Chem. A* **2008**, *112*, 11861–11872.
- (75) Muhammad, S.; Irfan, A.; Shkir, M.; Chaudhry, A. R.; Kalam, A.; Al-Faify, S.; Al-Sehemi, A. G.; Al-Salami, A. E.; Yahia, I. S.; Xu, H. L.; et al. How Does Hybrid Bridging Core Modification Enhance the Nonlinear Optical Properties in Donor- π -Acceptor Configuration? A Case Study of Dinitrophenol Derivatives. *J. Comput. Chem.* **2015**, *36*, 118–128.
- (76) Rawal, M.; Garrett, K. E.; Johnson, L. E.; Kaminsky, W.; Jucov, E.; Shelton, D. P.; Timofeeva, T.; Eichinger, B. E.; Tillack, A. F.; Robinson, B. H.; et al. Alternative Bridging Architectures in Organic Nonlinear Optical Materials: Comparison of π - and χ -Type Structures. *J. Opt. Soc. Am. B* **2016**, *33*, E160–E170.
- (77) Silva, D. L.; Fonseca, R. D.; Vivas, M. G.; Ishow, E.; Canuto, S.; Mendonca, C. R.; De Boni, L. Experimental and Theoretical Investigation of the First-Order Hyperpolarizability of a Class of Triarylamine Derivatives. *J. Chem. Phys.* **2015**, *142*, No. 064312.
- (78) Yuan, J.; Yuan, Y.; Tian, X.; Sun, J.; Ge, Y. Spirooxazine-Fulgide Biphotochromic Molecular Switches with Nonlinear Optical Responses Across Four States. *J. Phys. Chem. C* **2016**, *120*, 14840–14853.
- (79) Carlotti, B.; Cesaretti, A.; Cannelli, O.; Giovannini, T.; Cappelli, C.; Bonaccorso, C.; Fortuna, C. G.; Elisei, F.; Spalletti, A. Evaluation of Hyperpolarizability from the Solvatochromic Method: Thiophene Containing Push–Pull Cationic Dyes as a Case Study. *J. Phys. Chem. C* **2018**, *122*, 2285–2296.
- (80) Paschoal, D.; Santos, H. F. D. Computational Protocol to Predict Hyperpolarizabilities of Large π -Conjugated Organic Push–Pull Molecules. *Org. Electron.* **2016**, *28*, 111–117.
- (81) Corozzi, A.; Mennucci, B.; Cammi, R.; Tomasi, J. Structure versus Solvent Effects on Nonlinear Optical Properties of Push–Pull Systems: A Quantum-Mechanical Study Based on a Polarizable Continuum Model. *J. Phys. Chem. A* **2009**, *113*, 14774–14784.
- (82) Bale, D. H.; Eichinger, B. E.; Liang, W.; Li, X.; Dalton, L. R.; Robinson, B. H.; Reid, P. J. Dielectric Dependence of the First Molecular Hyperpolarizability for Electro-Optic Chromophores. *J. Phys. Chem. B* **2011**, *115*, 3505–3513.
- (83) Capobianco, A.; Centore, R.; Noce, C.; Peluso, A. Molecular Hyperpolarizabilities of Push–Pull Chromophores: A Comparison Between Theoretical and Experimental Results. *Chem. Phys.* **2013**, *411*, 11–16.
- (84) Vivas, M. G.; Silva, D. L.; Rodriguez, R. D. F.; Canuto, S.; Malinge, J.; Ishow, E.; Mendonca, C. R.; De Boni, L. Interpreting the First-Order Electronic Hyperpolarizability for a Series of Octupolar Push–Pull Triarylamine Molecules Containing Trifluoromethyl. *J. Phys. Chem. C* **2015**, *119*, 12589–12597.
- (85) Davydov, A. S. *Theory of Molecular Excitons*; Plenum Press: NY, 1971.
- (86) Agranovich, V. M. *Excitations in Organic Solids*; International Series of Monographs on Physics; Oxford University Press: Oxford, U.K, 2008; Vol. 142.
- (87) Kocherzhenko, A. A.; Sosa Vazquez, X. A.; Milanese, J. M.; Isborn, C. M. Absorption Spectra for Disordered Aggregates of Chromophores Using the Exciton Model. *J. Chem. Theory Comput.* **2017**, *13*, 3787–3801.
- (88) McRae, E. G.; Kasha, M. Enhancement of Phosphorescence Ability upon Aggregation of Dye Molecules. *J. Chem. Phys.* **1958**, *28*, 721–722.
- (89) Yamagata, H.; Maxwell, D. S.; Fan, J.; Kittilstved, K. R.; Briseno, A. L.; Barnes, M. D.; Spano, F. C. HJ-Aggregate Behavior of Crystalline 7,8,15,16-Tetraazaterrylene: Introducing a New Design Paradigm for Organic Materials. *J. Phys. Chem. C* **2014**, *118*, 28842–28854.
- (90) Ishizaki, A.; Fleming, G. On the Adequacy of the Redfield Equation and Related Approaches to the Study of Quantum Dynamics in Electronic Energy Transfer. *J. Chem. Phys.* **2009**, *130*, No. 234110.
- (91) Tillack, A. F.; Johnson, L. E.; Eichinger, B. E.; Robinson, B. H. Systematic Generation of Anisotropic Coarse-Grained Lennard-Jones Potentials and Their Application to Ordered Soft Matter. *J. Chem. Theory Comput.* **2016**, *12*, 4362–4374.
- (92) Frenkel, J. On the Transformation of Light Into Heat in Solids. I. *Phys. Rev.* **1931**, *37*, 17–44.
- (93) Frisch, M. J.; Trucks, G. W.; Schlegel, H. B.; Scuseria, G. E.; Robb, M. A.; Cheeseman, J. R.; Scalmani, G.; Barone, V.; Mennucci, B.; Petersson, G. A. et al. *Gaussian 09*, revision D.01; Gaussian Inc.: Wallingford, CT, 2013.
- (94) Hehre, W.; Ditchfield, R.; Pople, J. Self-Consistent Molecular Orbital Methods. XII. Further Extensions of Gaussian-Type Basis Sets for Use in Molecular Orbital Studies of Organic Molecules. *J. Chem. Phys.* **1972**, *56*, 2257–2261.
- (95) Hariharan, P.; Pople, J. The Influence of Polarization Functions on Molecular Orbital Hydrogenation Energies. *Theor. Chim. Acc.* **1973**, *28*, 213–222.
- (96) Chai, J.-D.; Head-Gordon, M. Systematic Optimization of Long-Range Corrected Hybrid Density Functionals. *J. Chem. Phys.* **2008**, *128*, No. 084106.
- (97) Krueger, B. P.; Scholes, G. D.; Fleming, G. R. Calculation of Couplings and Energy-Transfer Pathways Between the Pigments of LH2 by the Ab Initio Transition Density Cube Method. *J. Phys. Chem. B* **1998**, *102*, 5378–5386.

- (98) Lu, T.; Chen, F. Multiwfn: A multifunctional wavefunction analyzer. *J. Comput. Chem.* **2012**, *33*, 580–592.
- (99) Breneman, C. M.; Wiberg, K. B. Determining Atom-Centered Monopoles from Molecular Electrostatic Potentials. The Need for High Sampling Density in Formamide Conformational Analysis. *J. Comput. Chem.* **1990**, *11*, 361–373.
- (100) Kaminsky, W. WinTensor, 2014. <http://cad4.cpac.washington.edu/WinTensorhome/WinTensor.htm>.
- (101) Wampler, R. D.; Moad, A. J.; Moad, C. W.; Heiland, R.; Simpson, G. J. Visual Methods for Interpreting Optical Nonlinearity at the Molecular Level. *Acc. Chem. Res.* **2007**, *40*, 953–960.
- (102) Hauptert, L. M.; Simpson, G. J. Chirality in Nonlinear Optics. *Annu. Rev. Phys. Chem.* **2009**, *60*, 345–365.
- (103) Kittel, C. *Introduction to Solid State Physics*, 8th ed.; Wiley: Hoboken, NJ, 2014.
- (104) Jin, W.; Johnston, P. V.; Elder, D. L.; Manner, K. T.; Garrett, K. E.; Kaminsky, W.; Xu, R.; Robinson, B. H.; Dalton, L. R. CCDC 1446693: Experimental Crystal Structure Determination, 2016.